AUDITORY SYSTEM COMPARISONS BETWEEN SAND CATS AND OTHER FELID SPECIES:

ACOUSTIC INPUT ADMITTANCE OF EARS AND AUDITORY BRAINSTEM RESPONSES

By

Howard F. Chan

Submitted to the Department of Electrical Engineering and Computer Science

in Partial Fulfillment of the Requirements for the Degree of

Master of Engineering in Electrical Engineering and Computer Science

at the Massachusetts Institute of Technology

May 19, 2005 [June 2005]

Author _____
Department of Electrical Engineering and Computer Science
May 19, 2005

Certified by _____
William T. Peake
Thesis Supervisor, Professor of Electrical Engineering and Computer Science

Certified by _____
John J. Rosowski
Thesis Supervisor, Research Affiliate at the Research Laboratory for Electronics

Accepted by _____
Arthur C. Smith
Chairman, Department Committee on Graduate Theses

AUDITORY SYSTEM COMPARISONS BETWEEN SAND CATS AND OTHER FELID SPECIES:

ACOUSTIC INPUT ADMITTANCE OF EARS AND AUDITORY BRAINSTEM RESPONSES

by

Howard F. Chan

Submitted to the
Department of Electrical Engineering and Computer Science

May 19, 2005

In Partial Fulfillment of the Requirements for the Degree of
Master of Engineering in Electrical Engineering and Computer Science

ABSTRACT

The sand cat, one species of the cat family, is found only in deserts and has unusually large ear canals and middle-ear air cavities. Recent work has shown that sand cat ears absorb acoustic power at low frequencies (<1 kHz) better than those of domestic cats (Huang et al. 2002). In this thesis, we test this hypothesis by comparing acoustic input-admittance, which determines acoustic power absorption, and thresholds of auditory-brainstem responses. In a zoo, measurements were made in 37 ears of 23 anesthetized specimens, including sand cats and five other felid species. Sand cats have lower mean thresholds at frequencies between 0.25 and 5 kHz by 6-9 dB than other felid species measured. However, the mean power absorption does not differ significantly. The results are consistent with the hypothesis that sand-cat hearing is unusually sensitive, but this specialization is not associated with increased power absorbed at the tympanic membrane.

Thesis Supervisor: William T. Peake
Title: Professor, Research Laboratory for Electronics and Eaton Peabody Laboratory of Auditory Physiology

Thesis Supervisor: John J. Rosowski
Title: Research Affiliate, Research Laboratory for Electronics and Eaton Peabody Laboratory of Auditory Physiology

Acknowledgements

I would like to thank my advisors Professors Bill Peake and John Rosowski for their constant mentoring and advice on this work. Professor Peake's passion for understanding evolutionary processes as well as his insights and thoughtful criticism permeate this thesis. Professor Rosowski's keen knowledge of acoustics has helped me link the knowledge learned from books to actual applications. Both men have greatly influenced my approach to scientific curiosities.

I appreciate Kim Clark, Dr. Kevin Leiske, and the staff at The Living Desert Zoo and Gardens for making the time and providing the space for us to make measurements in the exotic felids.

This work would not have been possible were it not for the efforts of Edward and Michael Walsh, and JoAnn McGee for measuring auditory brainstem responses, which is a key component in linking auditory structures with function.

I would like to thank the Mike, Amanda, Jocelyn, Melissa, Saumil, and Wade in the Wallace Middle Ear group at the Eaton Peabody Laboratory at the Massachusetts Eye and Ear Infirmary. This work definitely benefited from the helpful feedback and different perspectives of each group member.

Lastly, I would also like to thank the National Institute of Health for proving the funding to make this work possible.

Table of Contents

Table of Figures

Table of Tables

1 Introduction

Changes in natural environments induce variations in the structures of creatures that live within them. When Charles Darwin explored the Galapagos Island, he found flora and fauna that were variations of the ones found on the continent of South America. Thirteen different species of finches were found on these islands, each species with a differently shaped beak. Some had flat-wide beaks that were used to crack nuts fallen down from trees while others had sharp-curved beaks used to pick out worms from tree bark. Other bird species had distinctively more "colorful" plumage than their mainland counterparts. Explanations proposed for these changes were differentiation in food gathering, competition in mating, selectivity due to predators, and pressures from habitat conditions (Darwin 1839).

These variations occur in different physiological systems, across different species, and within different habitats. In this thesis, we focus our efforts on specializations of anatomical structures and functions in the auditory system of species in the cat family (Felidae).

1.1 Adaptation

In evolutionary theory, adaptation refers to structural changes that produce a functional advantage that increases the rate of survival for a particular species within its niche. Knowledge of adaptive features in the auditory system may allow us to compare

variations in hearing performances across species. That is, isolated structural features (or a constellation) in a species can potentially be related to advantageous (i.e. adaptive) function.

1.2 Background

Research has shown that some desert species have specialized auditory structures that are thought to improve sensitivity to low frequencies sound (<1 kHz). Three examples are kangaroo rats (Webster and Webster, 1984), desert grasswrens (Schodde 1982), and sand cats (Huang et al. 2002). Each of these desert species has been shown to have unusual auditory structures compared to cousins within their families. Below is a short description of the anatomy and physiology of the auditory system. The description tries to provide basic knowledge of the auditory system and is meant to establish nomenclature that will be used for the rest of this thesis.

1.2.1 Anatomy and Physiology of the Ear

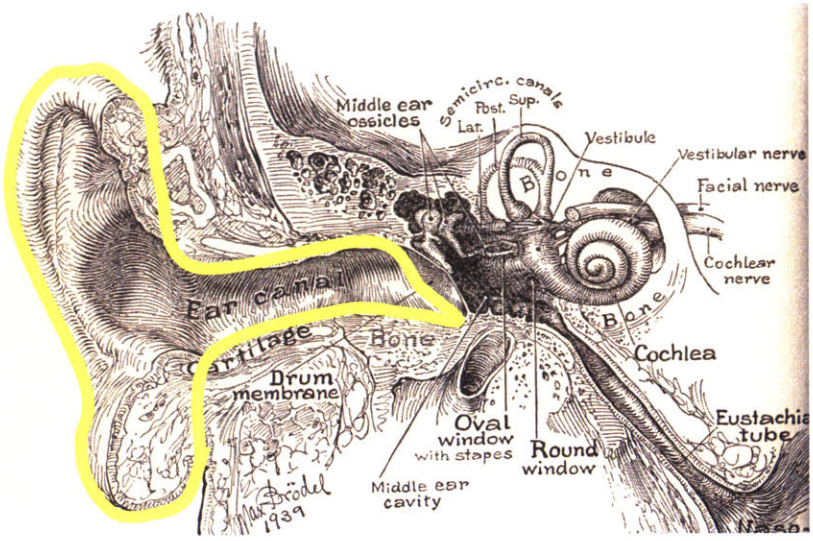

Figure 1.1: Picture of the human auditory system (from Wever and Lawrence 1954). The outer ear is highlighted.

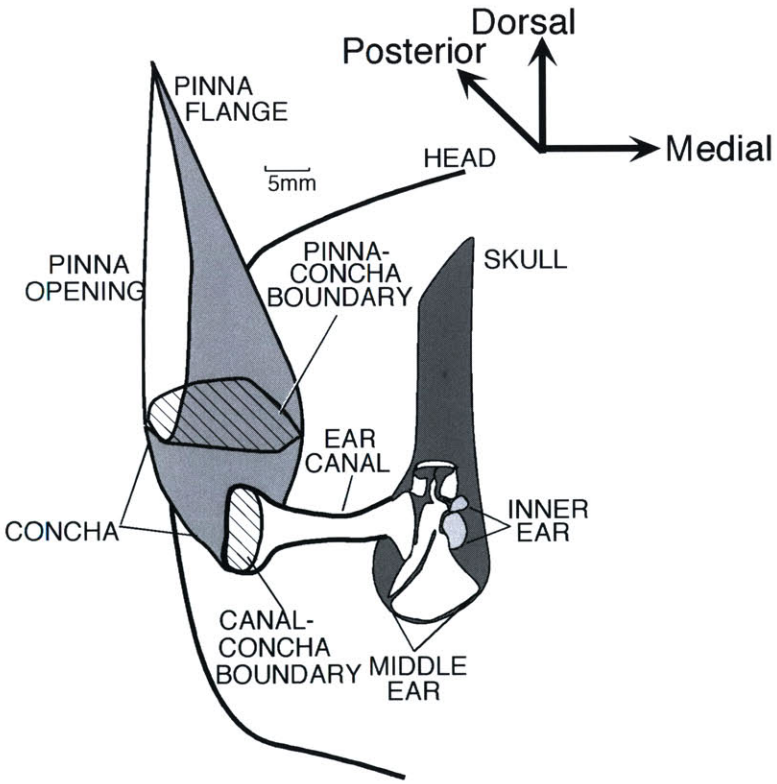

Figure 1.2: Schematic picture of structures in a felid ear (from Huang et al. 2002).

The ear can be divided into three regions: the outer, middle, and inner ear. The outer ear (Figure 1.1) consists of the pinna, concha, and external ear canal (EC). The pinna is the outer cartilaginous flap of the ear which surrounds a funnel-shaped recess known as the concha. The concha is attached to the external ear canal which couples to the tympanic membrane (TM), commonly known as the ear drum. In felid ears, the ear canal narrows starting from the concha and then makes an almost 90 degree turn medially (Figure 1.2). The ear canal widens as it reaches the tympanic membrane. The pinna collects sound and directs it through the concha and the external ear canal to the tympanic membrane. The sound pressure causes motion of the tympanic membrane.

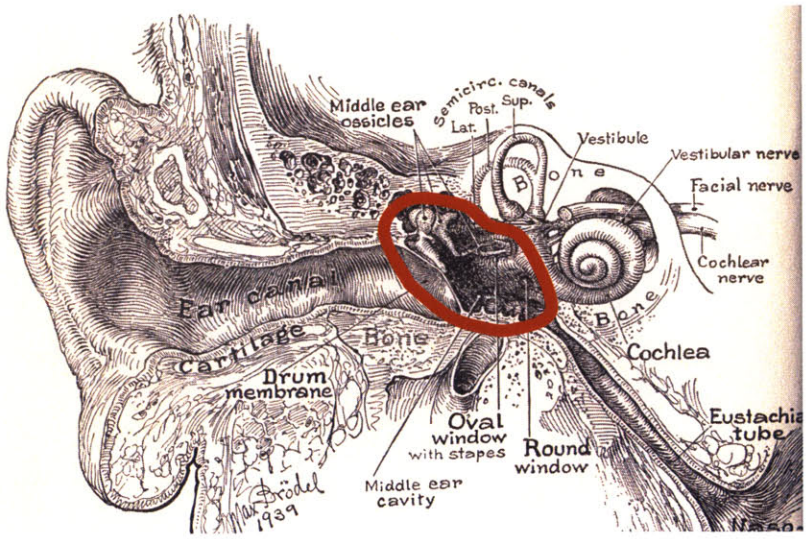

Figure 1.3: The middle ear is highlighted.

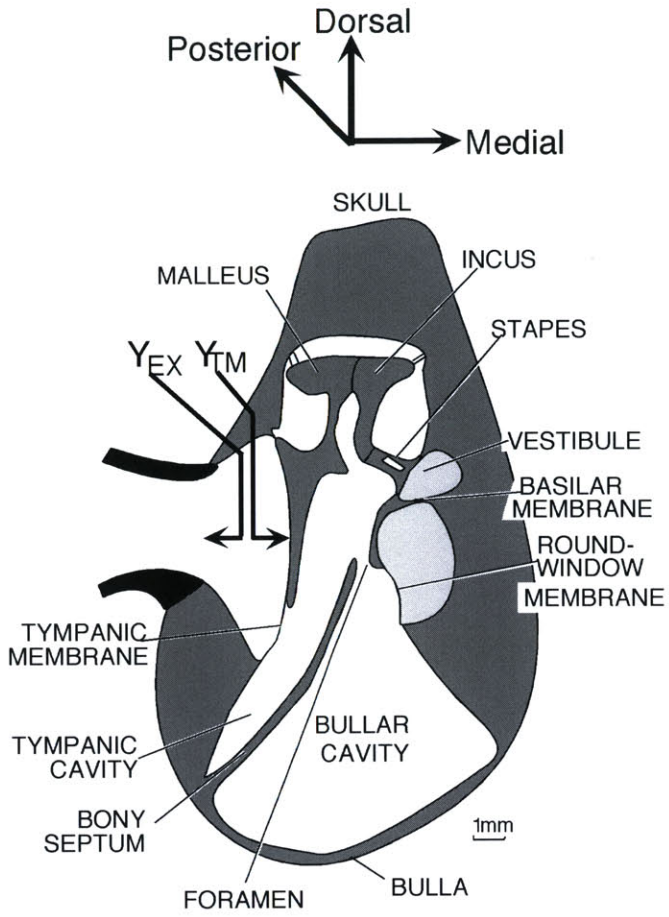

Figure 1.4: Schematic drawing of the middle ear of a domestic cat (from Huang et al. 2002).

The middle ear (Figure 1.3) is an enclosed air-filled cavity between the tympanic membrane (TM) and the oval window of the inner ear. The TM and oval window are linked by a chain of three ossicles. The ossicles - the malleus, the incus, and the stapes - are suspended in the middle-ear cavity by ligaments and the tympanic membrane. The tympanic membrane is attached to the manubrium, which is the long arm of the malleus. The malleus is in turn connected to the incus, which is connected to the stapes. The footplate of the stapes fits in the oval window. Middle ears in many mammals, such as rats and cats, are surrounded by bony walls known as the auditory bullae (Figure 1.4). Outward bulging of the auditory bullae increases the air volume in the middle ear. As

sound moves the tympanic membrane, vibration is turned into mechanical energy and is transferred through the three-ossicle chain. The force exerted by the footplate of the stapes pushes against the oval window.

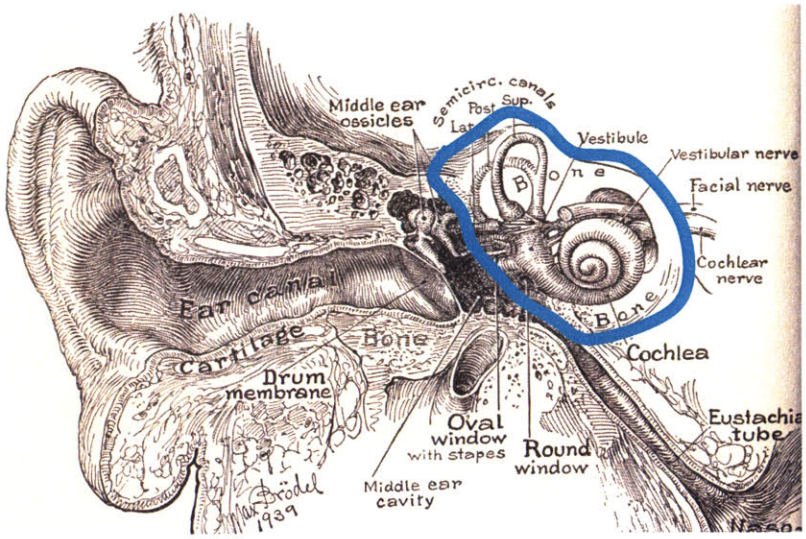

Figure 1.5: The inner ear is highlighted.

The auditory part of the inner ear (Figure 1.5) is the fluid-filled space enclosed in bone, where the cochlea resides. The cochlea is a spiral structure that contains the sensory transducer, the organ of corti. The organ of corti has specialized receptors that sense motion and form synaptic connections to the auditory-nerves fibers. The force exerted by the footplate of the stapes is transformed into fluid pressure and motion in the inner ear. Motion of the organ of corti produced by the motion of the stapes is detected by the hair cells in the cochlea. This mechanical stimulation produces a change in the electrical potential across the hair-cell membrane which causes release of a chemical transmitter from the hair cell. The transmitter excites the synaptic endings of nerve fibers that send electrical impulses through the auditory nerve into the brainstem.

1.3 Motivation

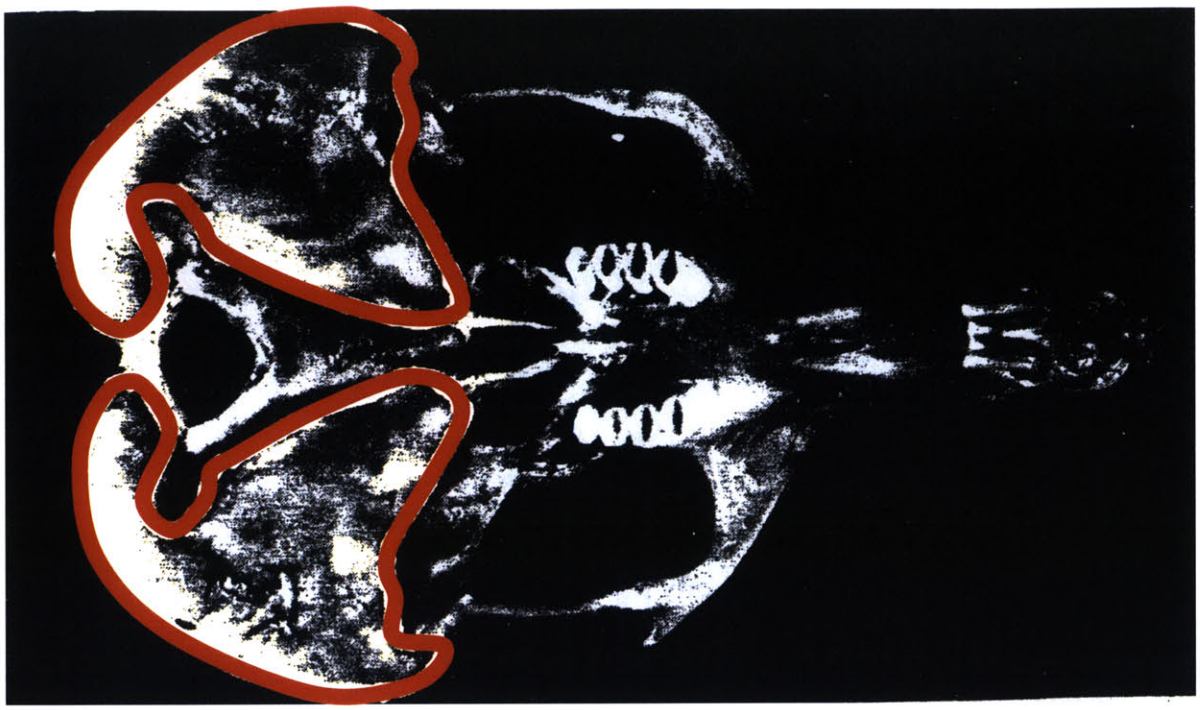

Figure 1.6: Ventral view of the skull of a kangaroo rat (Webster and Webster 1984). The red lines outline the auditory bullae. The volume of the auditory bullae is about twice that of the brain in this animal.

1.3.1 Past Work

Webster and Webster (1984) have shown that the kangaroo rat, which lives exclusively in the desert, has specialized outer, middle, and inner ear structures. Kangaroo rats have larger ear canal cross-sectional area and tympanic membranes, and most noticeably an enlarged auditory bulla (Figure 1.6). The combined volume of the right and left auditory bulla exceeds the volume of the brain case. These features have been shown to allow kangaroo rats to be sensitive to low frequency sound in their extreme desert habitat. Predators of the kangaroo rats, owls and snakes, produce a low frequency sound just as they attack their prey (Webster and Webster 1971). This sensitivity to low frequency

sounds has been demonstrated to increase chances of kangaroo rats evading their predators. When the bullae were opened and partially filled with clay to reduce the air volume of the bullae, the kangaroo rats had reduced sensitivity to low frequency sound and were more readily captured by their predators. The Websters (1972) conclude that desert species tend to have enlarged auditory bullae as an adaptive feature.

Fairy-wrens, whose habitat ranges from the rain forests of Papua New Guinea to the deserts of Australia, also have bony auditory bullae (Schodde 1982). Schodde observed that the size of the auditory bullae of each wren species increases as their habitats move to dryer and more open environment. The desert grasswrens, whose habitat is the Australian desert, have the largest auditory bullae among the species observed. Schodde conjectured that the swollen bullae allow detection of low-frequency sound which gives advance warning of incoming predators.

1.3.2 Recent Work

In this thesis, we look for similar ear adaptations to desert environment in the family Felidae. The "cat" family is suitable for studying function of the auditory systems because across species they (1) have similar behavioral characteristics, and (2) have similar middle-ear structures.

Felids are primarily nocturnal. As a consequence, hearing sensitivity is especially important to survival because it enables the detection of both prey and predators in their habitat. Felids, being primarily solitary and isolated animals, also rely on their ability to

transmit and detect sound in order to communicate with their conspecifics over long distances. One such instance would be a mother felid calling her kittens when food has been secured (Sliwa 1999).

The mostly uniform middle-ear structure in felid species allows a basis of comparison to unique specialized features. The presence of a bony septum divides the order Canivora into two suborders. The bony septum, which separates the tympanic cavity from the bullar cavity, is found in 4 families under the suborder Feliformia (which includes hyenas, mongooses, genets and civets, and felids) but is absent in other families in the suborder Caniformia (which includes dogs, bears, weasels, and raccoons (Wozencraft 1993)). Comparative studies on felid middle-ear have also concluded that the malleus is similar in term of structure across 29 felid species (Herrington 1986).

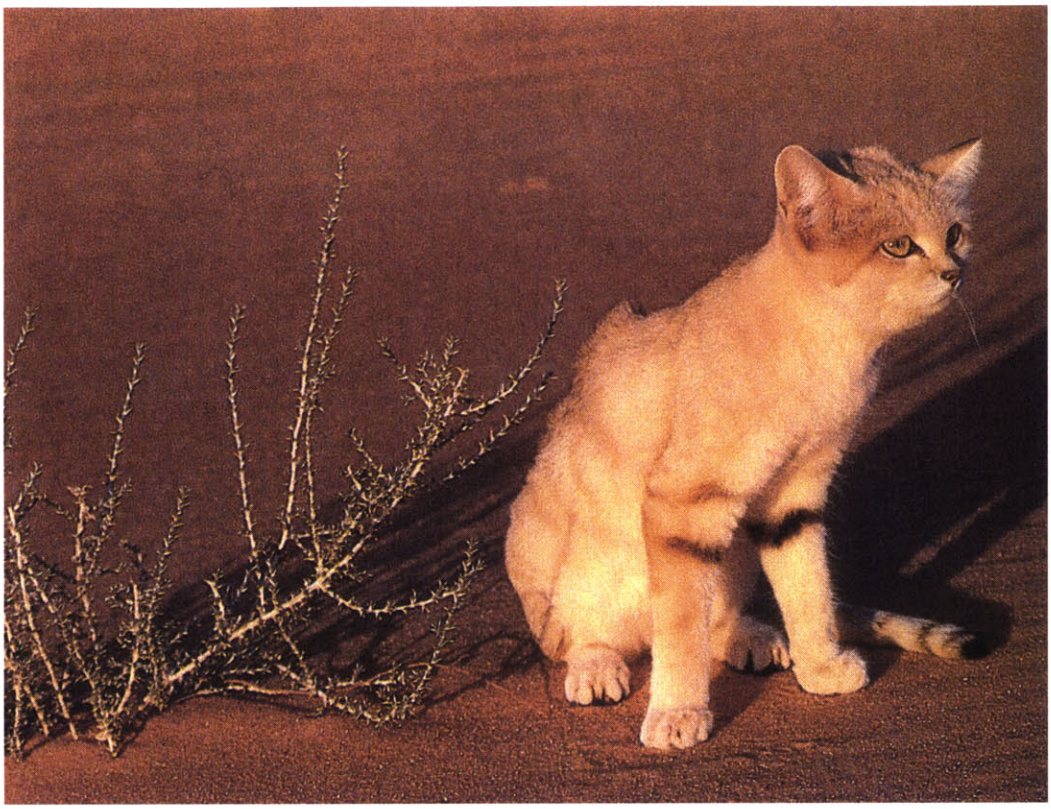

Figure 1.7: A sand cat in the Sahara desert (from Dragesco-Joffé 1993).

1.3.3 Sand cat

The sand cat (*Felis margarita*) (Figure 1.7) is a particular felid species that has been demonstrated to have specialized features of its ears, both structural and acoustic; these features have been theorized to be an adaptation to their habitat (Huang et al. 2002); the sand cat is the only felid species to live exclusively in deserts. Like kangaroo rats, sand cats have larger ear canal cross-sectional areas, tympanic-membrane areas, and middle-ear air volume in the auditory bulla relative to other cat species with similar body size. The average cross-sectional area of a sand cat's ear canal is just above three times the cross-sectional area of a domestic cat's ear canal. Similarly, sand cats' ear canals are on average twice the length of those measured in the domestic cats. The air volume within a

sand cat's auditory bulla is around 2 cubic centimeters, which is more than twice the air volume found in the bullae of domestic cats and Eurasian wildcats (Figure 1.8).

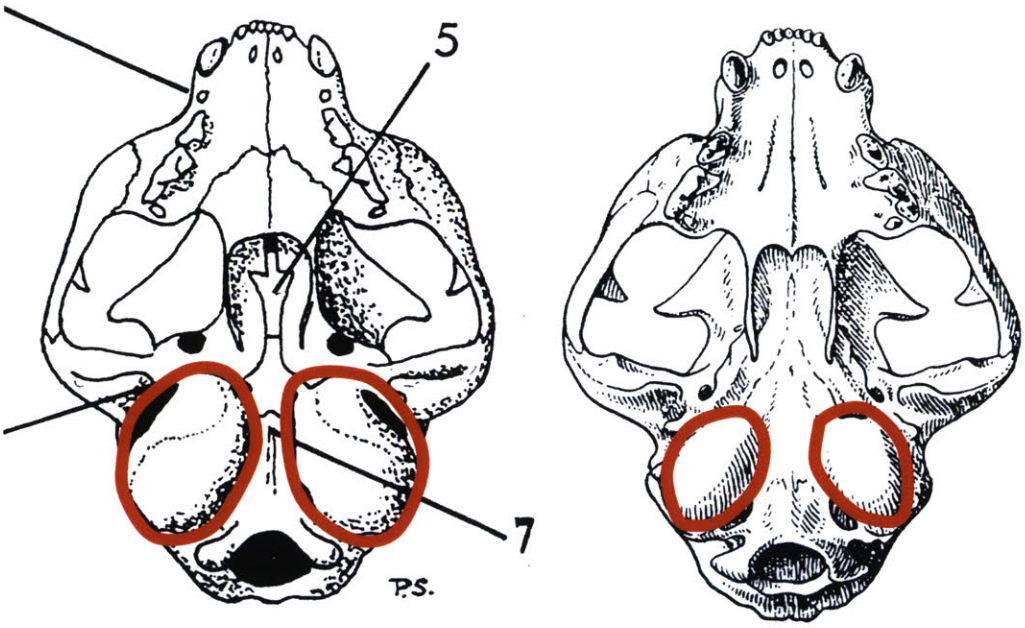

Figure 1.8: Drawings from ventral view of a sand cat skull (left) and a Eurasian wildcat (right). The auditory bullae are highlighted (from Peake and Peake, unpublished). The drawings are scaled to have the same length.

In Huang et al. (2002), sand cats' ears were shown to have mean acoustic input admittance that in magnitude is 5 times that of the domestic cat at low frequencies (<1 kHz). This feature and the configuration of the external ear imply that, with a diffuse sound field, sand cats' ears absorb more acoustic power at the tympanic membrane than is absorbed by domestic cats' ears at low frequencies. This difference in performance has been linked to acoustic results which show that low frequency sounds propagate better than high audio frequency in arid desert air.

Huang et al. (2002) assume that sand cats' superior ability to absorb acoustic power at the tympanic membrane provided greater sensitivity to sound at low frequencies. The theory assumes that the efficiency of power transmission through the middle ear, and the sensitivity of the inner ear and the central nervous system are equal across species. Thus, higher acoustic power absorbed at the input of the middle ear determines a lower hearing threshold for the detection of tones. In this thesis, we propose to test this hypothesis by comparing, in anesthetized specimens, measurements across some felid species of both acoustic input admittances at the tympanic membrane and hearing thresholds determined by electric responses of the auditory brainstem.

2 Methods

2.1 Overview: Two Kinds of Measurements

The acoustic admittance at the tympanic membrane, Y_{TM}, describes the ratio of the volume-velocity of the tympanic membrane (TM) and the ear-canal sound pressure that sets the TM into motion. Y_{TM} may indicate simple mechanical constraints on TM motion (e.g. compliant, viscous, or inertial) or some combinations of these. We measured Y_{TM} non-invasively in anesthetized cats of five species using a calibrated microphone-earphone system in a variant of the method described in Huang et al. (2000).

In the same animals, we estimated hearing thresholds using auditory brainstem responses (ABRs). The ABR is a sound-evoked electrical potential between the vertex of the cranium and the mastoid region behind the ear (Walsh et al. 1986). Edward Walsh, JoAnn McGee, and Michael Walsh from Boys Town National Research Hospital in Omaha, Nebraska recorded the auditory brainstem responses and determined the stimulus sound-pressure level for a threshold response.

2.2 Site of Data Collection

All measurements were made in the animal care hospital at The Living Desert Zoo and Gardens in Palm Desert, California between July 8th and 18th, 2004. At all times, the animal condition was under the direct supervision of the zoo's veterinarian. The animals were anesthetized via the inhalation of isoflurane gas, in order for the zoo' personal to do

their yearly physical exam. Our measurements were performed during and after the physical exams in 25 ears from 23 specimens from five felid species. No animals were harmed during the procedures which procedures followed the guidelines of the National Institute of Health.

2.3 Structural Measurements

We made measurements of the length, width, and depth of the heads of each animal using calipers. We also measured the three sides of the approximately triangular pinna of ears and recorded body weights. An otoscope was used to view the ear canal for wax and mites as well as to assess the health of the tympanic membrane. In some cases wax was removed. In most cases, TM was shiny and translucent. A cotton dam was then placed in the ear canal and hearing-aid mold material was injected to make an impression of the external ear from the pinna into the ear canal. After allowing a few minutes for the material to set, the elastic impression was removed. Measurements of the diameters of the elliptical cross-section of the ear canal were made from these impressions. In some ears, the mold material was not injected deeply enough to reach the ear canal. For these animals, diameters of the cartilaginous ear canal were estimated by uniform scaling of average measurements of bony ear canals from museum skulls of that species (Peake, personal communication). We assumed that the diameters of the bony ear canal exceed the diameters of the cartilaginous ear canal by a factor that is uniform across species. The scaling factor was determined as the ratio of averaged sand-cat cartilaginous ear canal radius (from ear molds) to sand cat bony ear canal radius (from museum skull) and was applied across species.

2.4 Acoustic Admittance

2.4.1 Approach

After removing the ear-canal impression, the eartip of a calibrated acoustic source (Figure 2.9) and microphone was sealed in the ear canal to measure admittance, Y_{EC}, at a point in the Ear Canal. Y_{EC} was measured with a series of different ear canal pressures in order to estimate the volume of the ear canal. This estimated volume and the measurements of the ear canal diameter were then used in a model of ear canal acoustics to calculate Y_{TM} from Y_{EC}. The method and tests of its accuracy and errors are reported in Huang et al. (2000b).

2.4.2 Hardware

Y_{EC} was measured using an acoustic system. The main component of this system was a commercially available acoustic source and microphone system, the Etymōtic Research ER10C. The ER10C, portable and powered by two 9V batteries, was connected to a Toshiba T2000SXE laptop with a signal processing card (DSP 16+). The sound source and microphone of the ER10C were coupled to a custom made assembly of two polyethylene tubes between 100 and 160 mm long with inner diameter of 0.76 and 1.57 mm, respectively. The tubes were held parallel by a elastic conical tip molded from silicone (RTV 6B) (Figure 2.1, 2.5). The microphone tube extended 3-4 mm beyond the end of the earphone tube in order to reduce the effects of evanescent, non-uniform modes generated at the earphone port on the measured sound pressure (Kinsler et al. 1982, page 216-222; Huang et al. 200b, page 1137). The assembly of the tubes and tip is called the

"eartip." A custom feature of our ER10C is a connecting tube that allows the eartip to be coupled to a syringe and a manometer used to control and monitor the static pressure in the ear canal (Huang et al. 2000). The computer generated a train of 40 ms long multi-frequency chirps that was used to drive the sound source, and simultaneously averaged the microphone output voltage synchronized to chirp onset. The responses of two hundred to one thousand chirps were averaged (to increase the signal-to-noise ratio) to determine the sound pressure in the ear canal. The sound source "calibration" was then used to convert the measured microphone voltage to admittance.

2.4.3 Calibration: Determination of Norton Equivalent circuit, Y_S and U_S

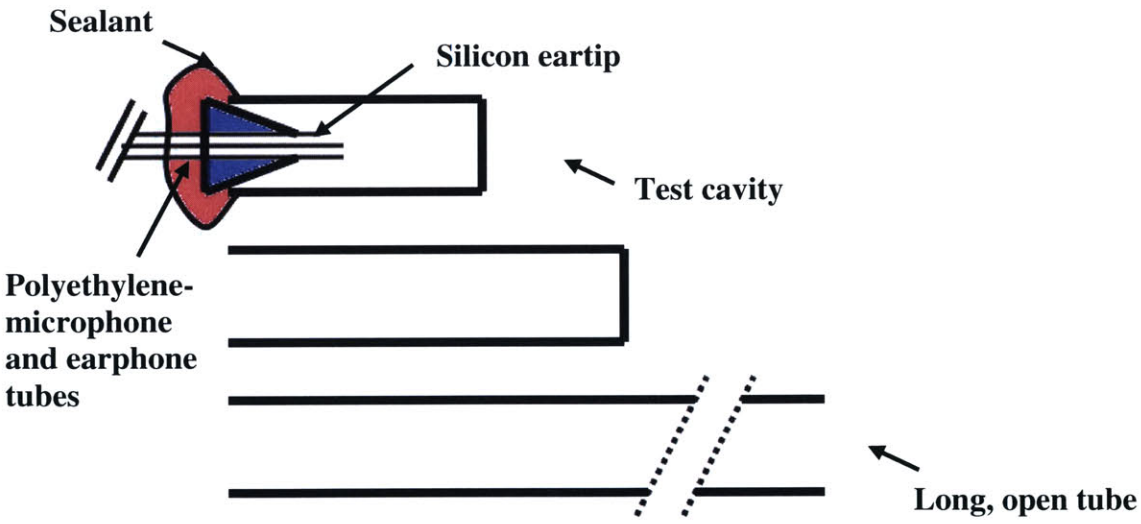

Figure 2.1: Calibration of eartip. The elastic eartip was inserted into a cavity or the long tube and sealed with pink ear-mold material. The measurement made in the short cavity (top) and the long tube (bottom) were used to characterize the Norton Equivalent circuit of the sound source. Measurements in the medium cavities (middle, only one is depicted here) were used to test the accuracy of the admittance measurement system.

Before load admittance can be determined from the microphone output, the acoustic source must be "calibrated" by measuring the microphone output in acoustic loads whose admittance is known. Each eartip was inserted into several rigid Plexiglas cylindrical cavities with rigid terminations and into a long tube, which was open at its distal end (Figure 2.1). The four cavities (labeled Cavity A, B, C, and D) varied in length from 8.1mm to 45.5 mm, respectively. The inside diameters of the four cavities varied between 5.5-7 mm. The inside diameter of the 10m long tube was about 6 mm. After placing the eartip some distance into each cylinder, the tip was sealed in place with ear mold material (Figure 2.1). A train of chirps was delivered through the ear tip and the microphone response was averaged, recorded, and Fourier transformed. In the case of the rigidly terminated cavities, the distance, L_{TUBE}, from the tip of the microphone tube to the rigid end of the cylinder was measured using a caliper. A "calibration set" consisted of measurements in one short cavity (A or B), two medium length cavity (C and D) and the long tube.

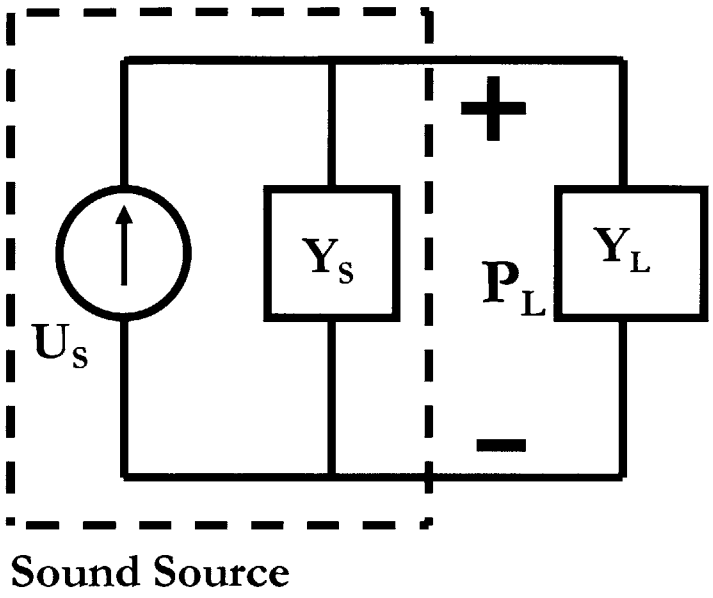

Figure 2.2: The sound source modeled as a Norton equivalent circuit. The microphone output is proportional to the pressure in the ear canal, P_L; Y_L is the admittance of the acoustic load into the eartip is sealed.

The acoustic source was characterized as a Norton equivalent circuit (Huang et al. 2000) with an ideal volume-velocity source, U_S, in parallel with source admittance, Y_S. These quantities ($U_S(f)$ and $Y_S(f)$) were determined from "calibration" measurements in the short cavity and long tube (Figure 2.2). These loads were described by a lossless, uniform tube model of 3.05 mm, an average of the cavity inner radii, and the length from the eartip to the rigid or open termination.

2.4.4 Tests of Measurement Accuracy

2.4.4.1 Comparison of Theory to Measurement

To test the accuracy of the system, the theoretical admittance of the intermediate cavities was calculated and compared with the admittance inferred from the measurements in the cavities. The comparisons show that our acoustic system is able to measure acoustic

admittance accurately up to 5 kHz (Figure 2.3). At frequencies higher than 5 kHz, difference between theory and measurement, even excluding the differences at sharp maxima and minima, are greater than 20%.

2.4.4.2 Sources of Error

Acoustic reasons for these large errors include effects of "crosstalk" from the earphone ports as well as electrical artifacts from within the ER10C earphone-microphone assembly itself. Acoustically, the extension of the microphone tubes enables the acoustic system to measure the load accurately at low frequency; however, at high frequencies, prediction errors are still present because the wavelengths at high frequencies are shorter than the microphone extension. Electrical artifacts of the acoustic system were measured by plugging both the microphone and earphones tubes. At high frequencies, the microphone output of the ER10C was not with measurement.

The system measured accurately at low frequencies and the errors increased at high frequencies. The comparisons, such as Figure 2.3, were used to select the upper limit of acceptable accuracy. Data of each individual ear is discarded at the frequency where the admittance magnitude and angle of the measured load are not accurately predicted by the theoretical load. For example, in Figure 2.3, data are deemed unreliable when the difference between the measured and the theoretical admittances are greater than 20%, which occurs at 5 kHz.

2.4.4.3 Difference in Frequency Limit from Huang et al. (2000)

In Huang et al. 2000, admittance results had an upper frequency range of 8 kHz, however, in our measurements, we found that our acoustic system generally can only predict data accurately up to 5 kHz. The reasons for this reduction in upper frequency limit could include an increase in electrical coupling from earphone input to microphone output, which has increased since the Huang et al. (2002) measurements because of degradation of insulation in the ER10C container.

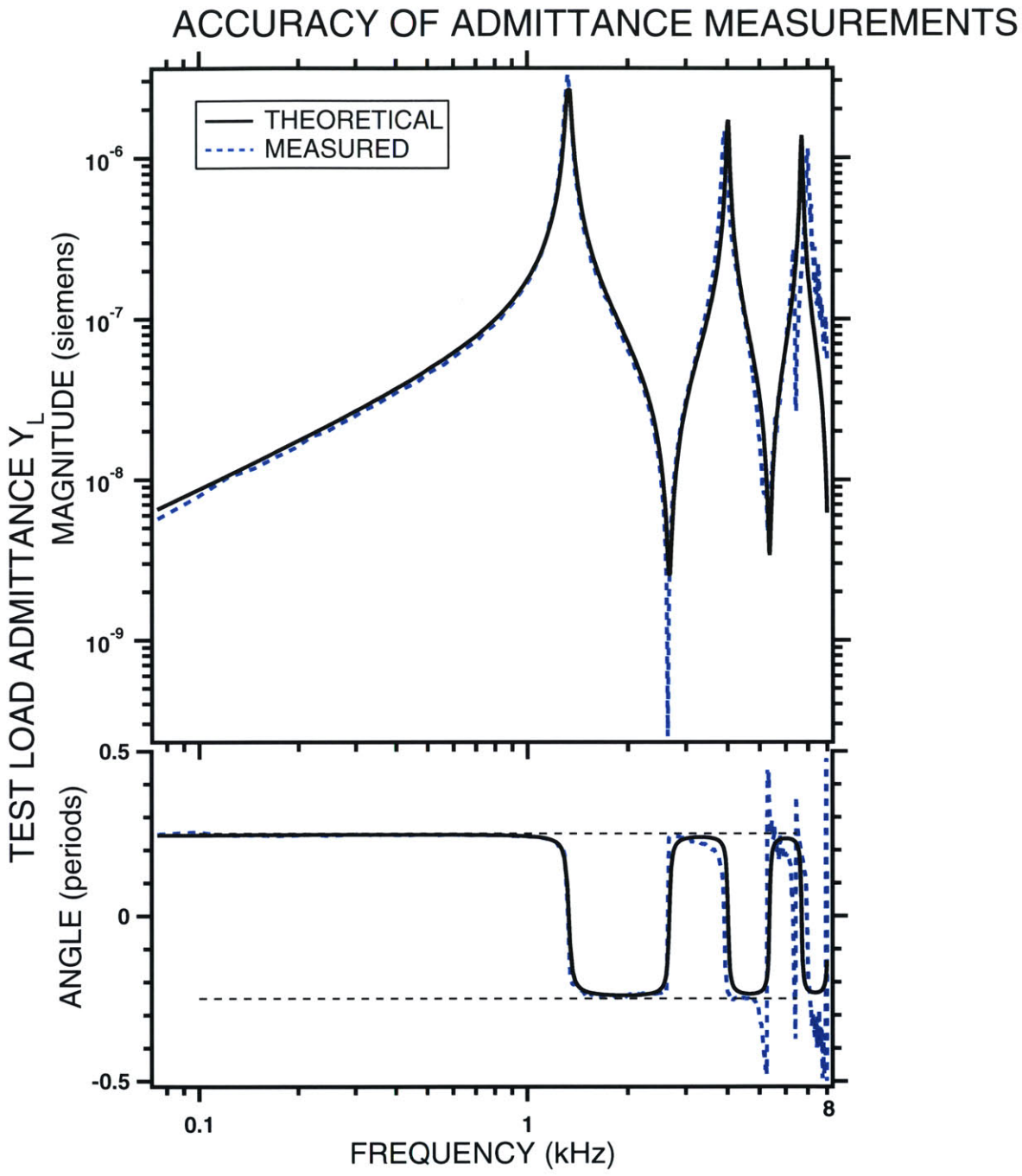

Figure 2.3: Comparison between theoretical and measured admittance. The test load is a rigidly terminated cavity with an inner diameter of 6.1 mm (Cavity E). The theoretical and calculated admittance magnitude, excluding regions of extreme maxima and minima, matches within 20% at frequencies below 6 kHz. The data presented in this thesis are restricted to the frequency range of 75 Hz – 5 kHz because for higher frequencies, the admittance measurements in test loads have large errors.

2.4.5 Effects of Variations in Eartip Construction on Y_S and U_S

2.4.5.1 Anatomical Constraints

In felids, the outer ear can be divided into three segments: pinna flange, concha, and ear canal (Figure 2.4). The concha funnels downward and then anteriorly from the pinna flange to the ear canal forms a backward 'J' shape. The concha narrows and bends medially towards the tympanic membrane to connect with the ear canal at the bend. The ear canal in domestic cats is narrowest midway between the canal-concha border and the tympanic membrane (Rosowski, Carney, and Peake 1988). This anatomy places constraints on the length and diameter of the eartip which should be small enough and flexible enough to slide into the canal, and wide enough, at its wider end, to fill the canal so that sound is delivered only to the ear canal load.

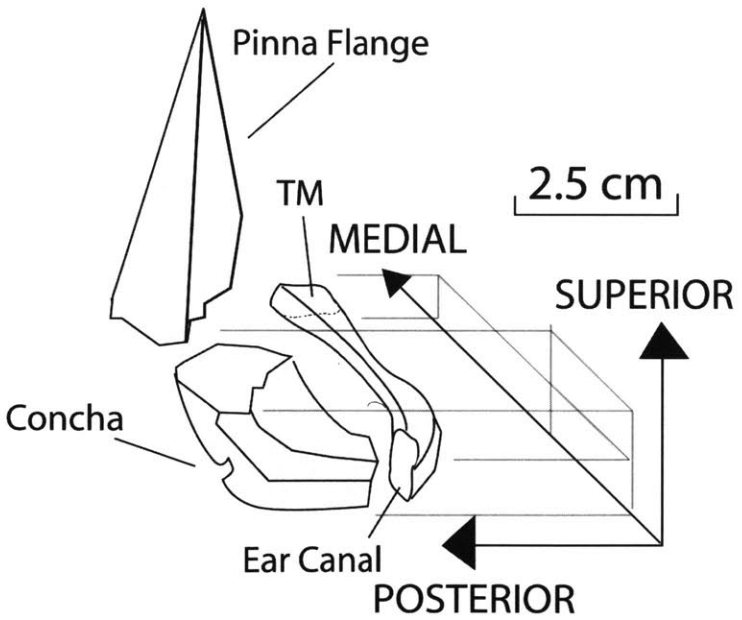

Figure 2.4: Exploded view of domestic cat's outer ear. The cartilaginous outer ear is separated into three parts: pinna flange, concha, and ear canal. At the concha-ear canal junction, there is a bend of almost 90 degrees medially inward towards the tympanic membrane. The concha connects to the ear canal at the bend. (Adapted from Rosowski, Carney, and Peake 1988)

2.4.5.2 Tube Length

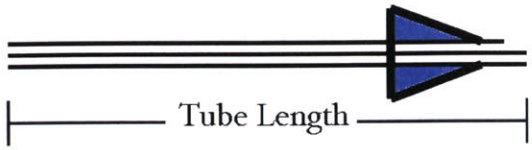

Figure 2.5: Eartip Tubes. "Tube length" is defined as the length of the microphone tube.

The polyethylene tubes (Figure 2.5) that we adopted for the eartip are 3 to 4 times longer than those used by Huang et al. (2000, page 1137): 100 to 160 mm versus 35 mm. The old shorter tubes made placement of the tip into the deeper ears of some species difficult; the new longer tubes made it easier both to insert the probe tip into the ear canal and to hold it in place during injection of the ear-mold sealant.

Lengthening the tubes altered the Norton equivalent admittance of the source (Figure 2.6). The magnitude of Y_S at low frequencies was increased by about a factor of 2 as one might expect because of the increased volume in the eartip; and the octave downward shift of $|Y_S|$ between Eartip A and Eartip B is consistent with a length dependent quarter-wave length resonance. $|U_S|$ also has a peak that moves down about an octave from Eartip A to Eartip B (Figure 2.6)

Although an increase in $|Y_S|$ with Eartip B makes it difficult to measure lower admittance loads accurately, sources with longer tubes are capable of accurate measurements of the test loads measured as part of our calibration process. Our acoustic sources can accurately measure loads up to 5 kHz (Figure 2.3).

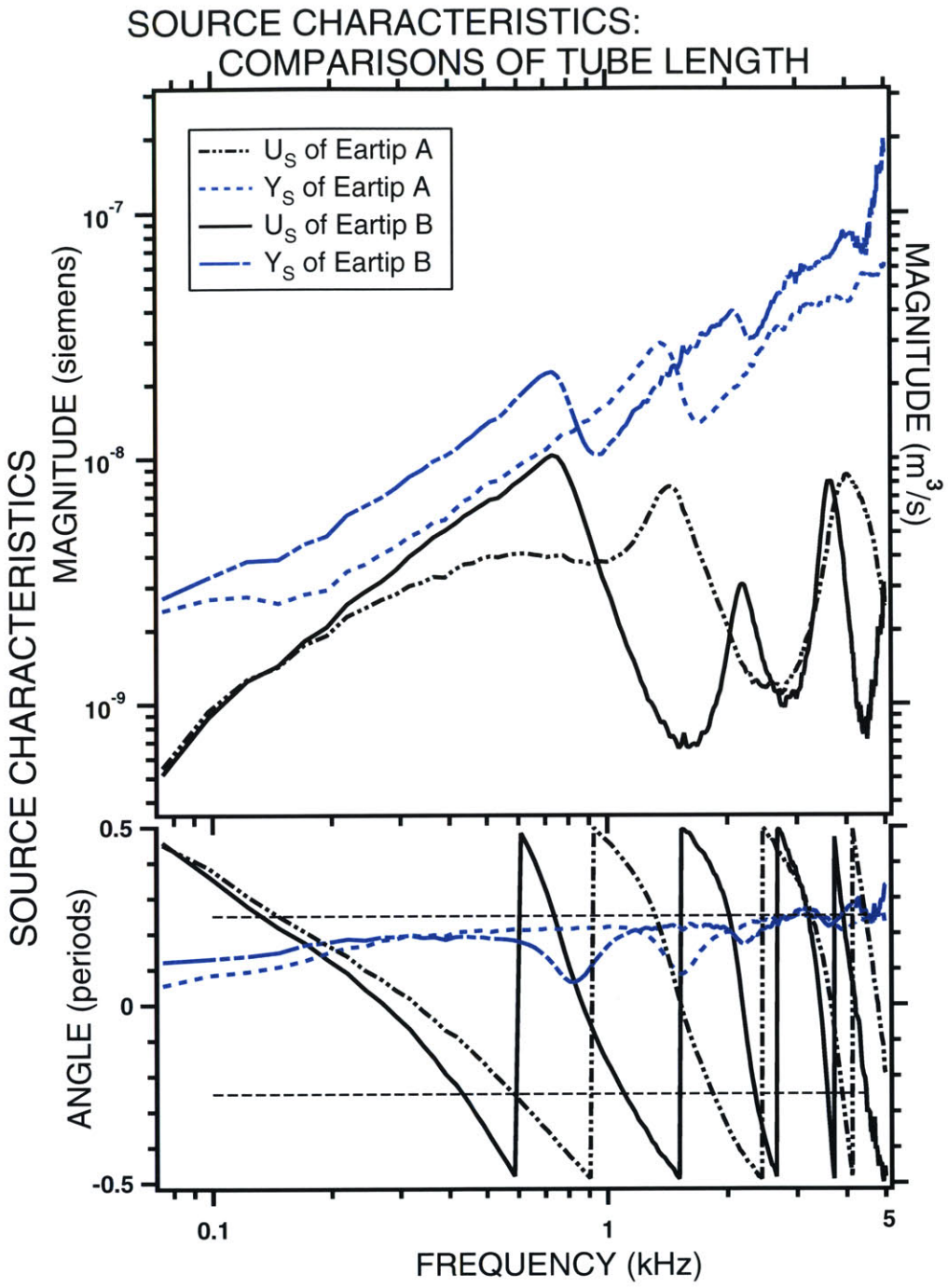

Figure 2.6: Effects of variations in tube length. The source admittances of two eartips, Y_S, with different length tubings are plotted. The comparison includes Y_S from an ear tip with tubes of 56 mm (Ear tip A) and an eartip of twice that length 114 mm (Ear tip B). The latter tube length was about the average the length of the ear tips used in this work. Both $|Y_S|$ and $|U_S|$ of Eartip B have roughly an octave shift to lower frequencies for peaks in $|Y_S|$ and $|U_S|$ relative to Eartip A, which indicates a length dependent resonance.

2.4.5.3 Tip Size

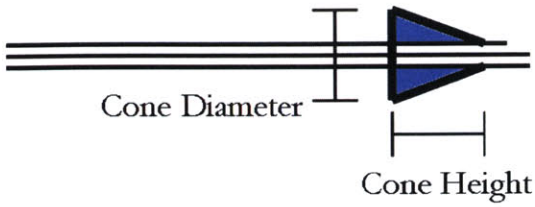

Figure 2.7: Eartip Cone Dimensions

The cone-shaped silicon tips we used are smaller in both diameter and length than those used by Huang et al. (2000). The diameter of the cone at its larger end was reduced by 30%, from an average of 8-9 mm to 6 mm. The height of the cone was reduced by 40%, from an average of 16-17 mm to 10-11 mm. This smaller tip allowed easier insertion into ears of species such as caracal, Arabian wildcat, and bobcats, which have narrower canals than sand cats.

Reducing the dimensions of the cone produces a small effect on Y_S (Figure 2.8). At low frequencies, the admittance magnitude of the source admittance with the smaller cone is about 10% less than the admittance with the larger cone. At high frequencies, $|Y_S|$ of the smaller cone eartip is about 40% smaller than the $|Y_S|$ with larger cone eartip. Reducing the dimensions of the cone has almost no effect on U_S at frequencies below 4 kHz.

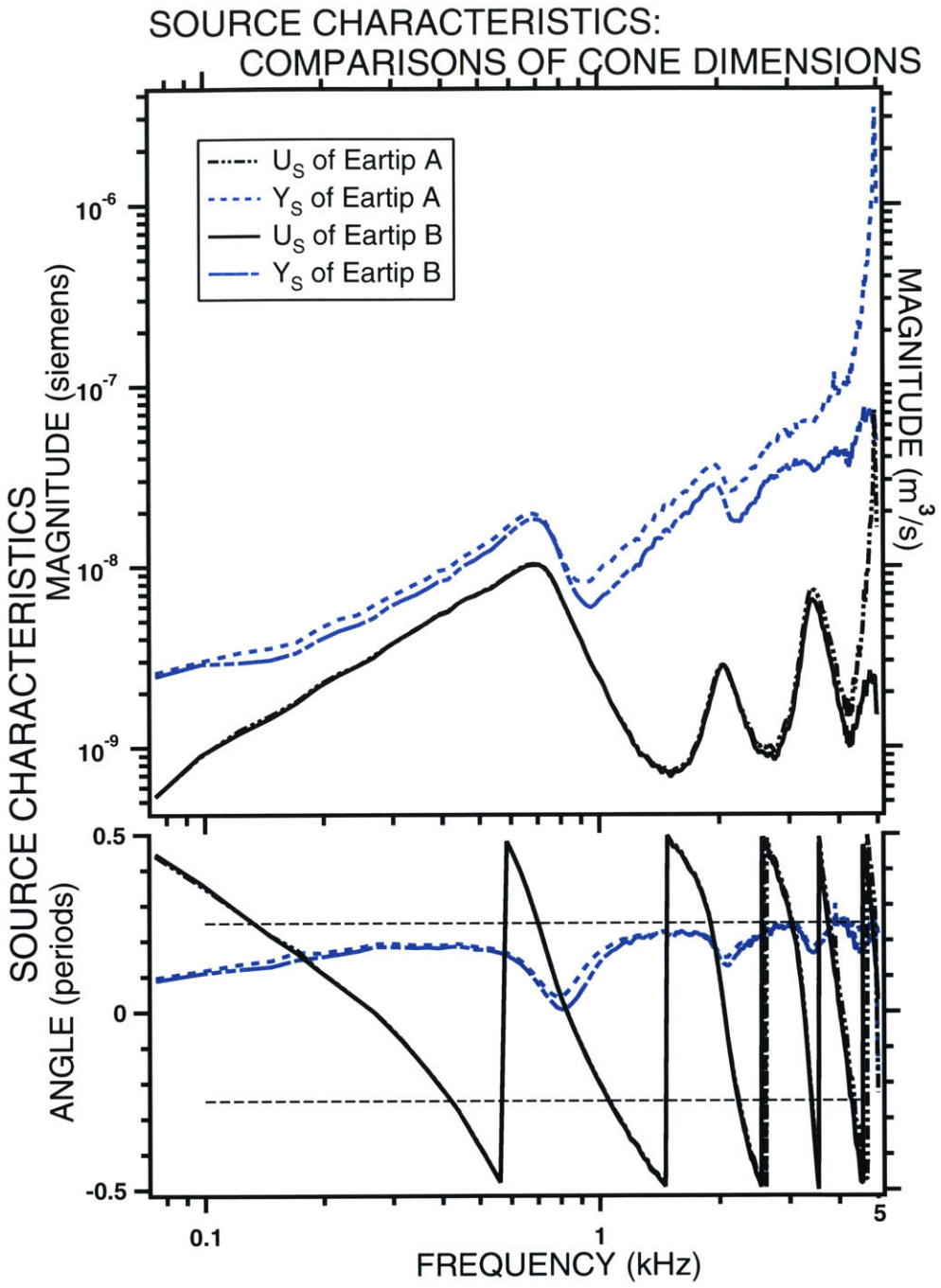

Figure 2.8: Effects of reduction in cone dimensions. The source admittances, Y_S, of two eartips with different cone dimensions are plotted. The comparison is made between an eartip with a cone 16.7 mm in length and 8.64 mm in diameter (Eartip A) and a smaller cone 10.5 mm in height and 6.3 mm in diameter (Eartip B). The figure shows that, at frequencies below 1 kHz, the two source admittances match each other within ±6% difference in magnitude. At high frequencies, Eartip B has smaller source admittance magnitude than Eartip A.

2.4.6 Measurements of Y_{EC}

The calibrated eartip was inserted into the ear canal. In order to seal the eartip in the canal, ear-mold material was injected into the ear canal, behind the eartip (Figure 2.9). Subsequently, periodic low-frequency sounds associated with body motion, such as breathing, seen in the microphone output (via an oscilloscope) were taken as a sign of a tight seal. Once the mold material was set, a chirp train was initiated. Y_{EC} was determined from the response recorded by the microphone with U_S and Y_S determined by calibration measurements with each eartip.

After measurements were completed, the ear mold with the embedded acoustic source and eartip were removed from the ear. The mold was assessed to estimate the location of the eartip in the ear canal as well as to determine how well the sealant surrounded the cone of the eartip as to isolate the medial ear canal from airspaces lateral to the cone.

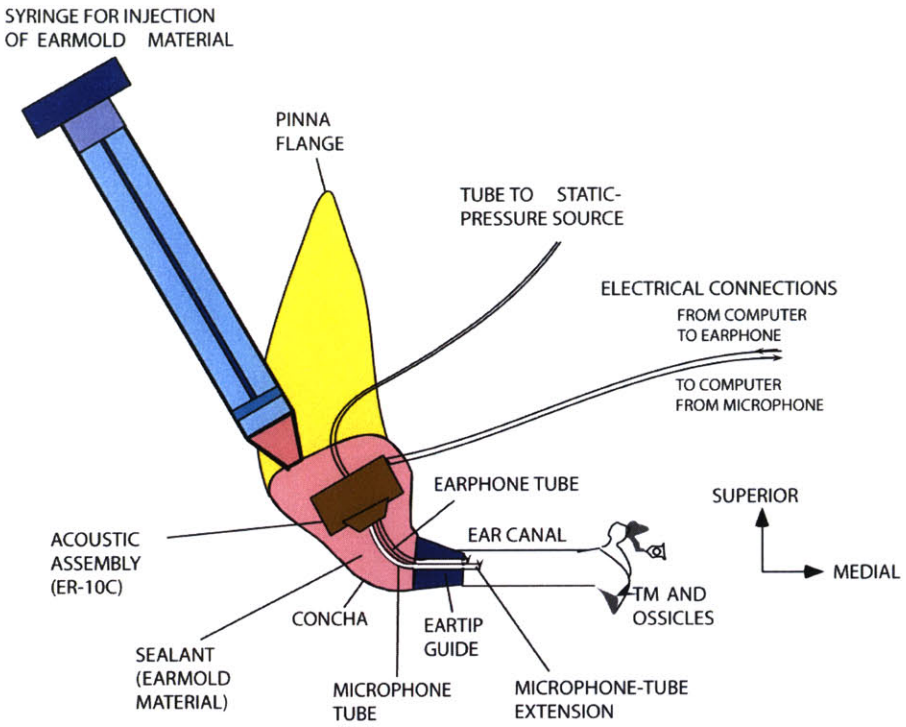

Figure 2.9: Insertion of the eartip into felid ear canal. The eartip was generally located close to the ear canal entrance and sealed with pink ear-mold material. Y_{EC} is the admittance inferred at the tip of the microphone tube (Huang et al. 2000b).

2.4.7 Tympanogram

Microphone responses with a fixed electric input to the earphone were recorded with different static pressures in the ear canal. Our standard sequence was to do a negative pressure series first in which responses were measured at static pressures of 0, -2, -5, -10, -20, -30 cm H_20. The static pressure was then returned to room pressure. Usually three or four measurements (over approximately two minutes) were made at 0 cm H_20 because it took time for the response to return to its original values. (Presumably, this effect was a consequence of the tympanic membrane's slow return to its original elastic state.) Next, positive pressure series responses were measured at 0, +2, +5, +10, +20, +30 cm

H_20. Finally, more measurements were made at 0 cm H_20 to test whether the system (including the tympanic membrane) returned to its initial state.

Tympanograms are plots of acoustic compliance at the ear tip, Y_{EC}, versus the static pressure in the ear canal for a low frequency; one was constructed from each pair of negative and positive pressure series. At each static pressure level, acoustic compliance, C_{EC}, was calculated from the averaged $\mathrm{Im}\{Y_{EC}(f)\}/(2\pi f)$ at 10 equally spaced points between 0.1 kHz to 0.3 kHz, a frequency range where ear admittances are primarily compliance-like.

These tympanograms were used to gauge the health of individual ears by assessing normality of the tympanic membrane's responses to change in static pressure. Ears that had tympanograms with unusual features were excluded from the analysis. Acoustic measurements of ears with tympanograms that met the acceptance criteria were used to determine the contribution of the ear canal between the source and the TM to the measured admittance.

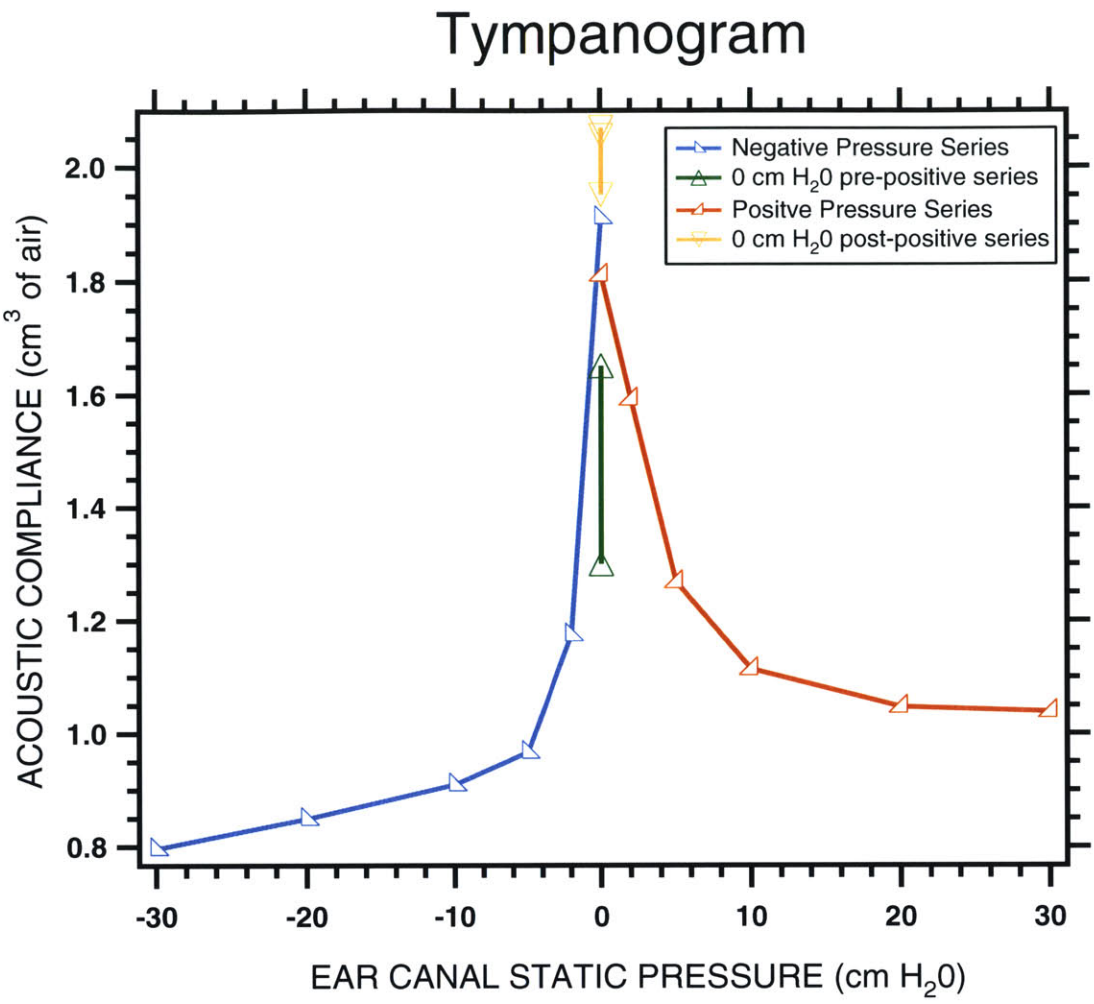

Figure 2.10: Tympanogram of the right ear of 404018, a one-year old female sand cat. At each static pressure level, acoustic compliance was calculated from the average of $\mathrm{Im}\{Y_{EC}(f)\}/(2\pi f)$ at 10 equally spaced points between 0.1 kHz to 0.3 kHz, the frequency range in which admittances were approximately compliance-like. A normal tympanogram exhibits an asymmetric, inverted "V" shape. Both negative and positive pressures decreased the compliance asymptotically. Repeated measurements were made with zero pressure after each pressure series to allow the tympanic membrane return to normal; usually, the response at 0 cm H_20 returned towards its initial values within the span of a few minutes. The key first indicates the sequence in which 4 subparts of the measurement were made. The triangles indicate measurements and each point towards the next static pressure measurement.

Acceptance Criteria for "valid" tympanograms:

Over-all Shape

In a tympanogram of a "normal" ear, acoustic compliance has an inverted "V" shape. Acoustic compliance increases as negative static pressure increases towards zero and reach its maximum value at ambient pressure. Acoustic compliance decreases as static pressure increase above 0 mm H_20 to positive static pressures. In some ears, the maximum acoustic compliance value occurred at +5 mm H_20. An explanation for this shift in maximum value could be that the inhalation of anesthesia had built up some positive pressure in the middle ear, thus resulting in a difference between ambient pressure and the pressure in the ear. For our results, acoustic admittance, Y_{EC}, is calculated at the static pressure where the maximum compliance occurs.

Asymmetry

Acoustic compliance for acceptable ears has an asymmetric decrease about the maximum compliance value. The compliance decreases more for the negative than positive pressure.

Asymptotic Behavior

Starting from the maximum value of the acoustic compliance, the compliance for the negative pressure series decreases rapidly and then more slowly as the pressure becomes more negatively we call this "asymptotic" pressure dependence. "Acceptable" asymptotic behavior is a decrease in slope between each static pressure point as pressure

moves away from ambient pressure. The compliance value at -30 cm H_20 in each tympanogram is required to be at least 20% below the compliance value at -20 cm H_20.

The asymptotic behavior of the positive series is more difficult to fit into a criterion. It was difficult to maintain the pressure seal for pressure above +20 cm H_20. Therefore, our rule was that acoustic compliance of acceptable ears decrease monotonically from the maximum value as static pressure increase until the pressure seal was broken. "Acceptable" asymptotic behavior of compliance values for both positive and negative series was determined by visual inspection of the tympanogram.

2.4.8 Calculation of Y_{TM}

2.4.8.1 Volume Calculation

The volume of air between the ear tip and the tympanic membrane can be estimated from the tympanogram at large negative static pressure levels where it is assumed the admittance magnitude at the TM has become small relative to that of the canal space. For volumes that are small compared to sound wavelength the following relationship describes the acoustic compliance's dependence on the volume,

$$Volume = Compliance(f) * (\rho_0 c^2),$$

where ρ_o is the density of air and c is the speed of sound in air. Thus, the acoustic determination of compliance (which is not dependent on frequency for the region chosen) allows computation of air volume.

2.4.8.2 Y_{TM}, the Acoustic Admittance at the Tympanic Membrane

Y_{TM} can be estimated by a transformation of Y_{EC} (Figure 2.11) using the distance between the ear tip and tympanic membrane, L_{EC} and assuming a simple model of a uniform tube. The distance from the ear tip to the tympanic membrane can be inferred from the air volume between the ear tip and the tympanic membrane and the area of the ear canal measured from the ear mold impression, i.e. $L_{EC} = V_{EC}/A_{EC}$. Modeling the ear canal as a lossless, uniform tube line, Y_{EC} can be transformed into Y_{TM} using the following:

$$Y_{TM} = Y_0 \frac{Y_{EC} - jY_0 \tan(kL_{EC})}{Y_0 - jY_{EC} \tan(kL_{EC})},$$

where Y_{EC} is the admittance measure at the eartip; $Y_0 = A_{EC}/(\rho_0 c) = \pi a^2/(\rho_0 c)$ is the specific acoustic impedance of air, L_{EC} is the length from the eartip to the tympanic membrane, $k = 2\pi f/c$ is the wave number, ρ_0 is the density of air, c is the propagation velocity of sound in air, and f is the frequency.

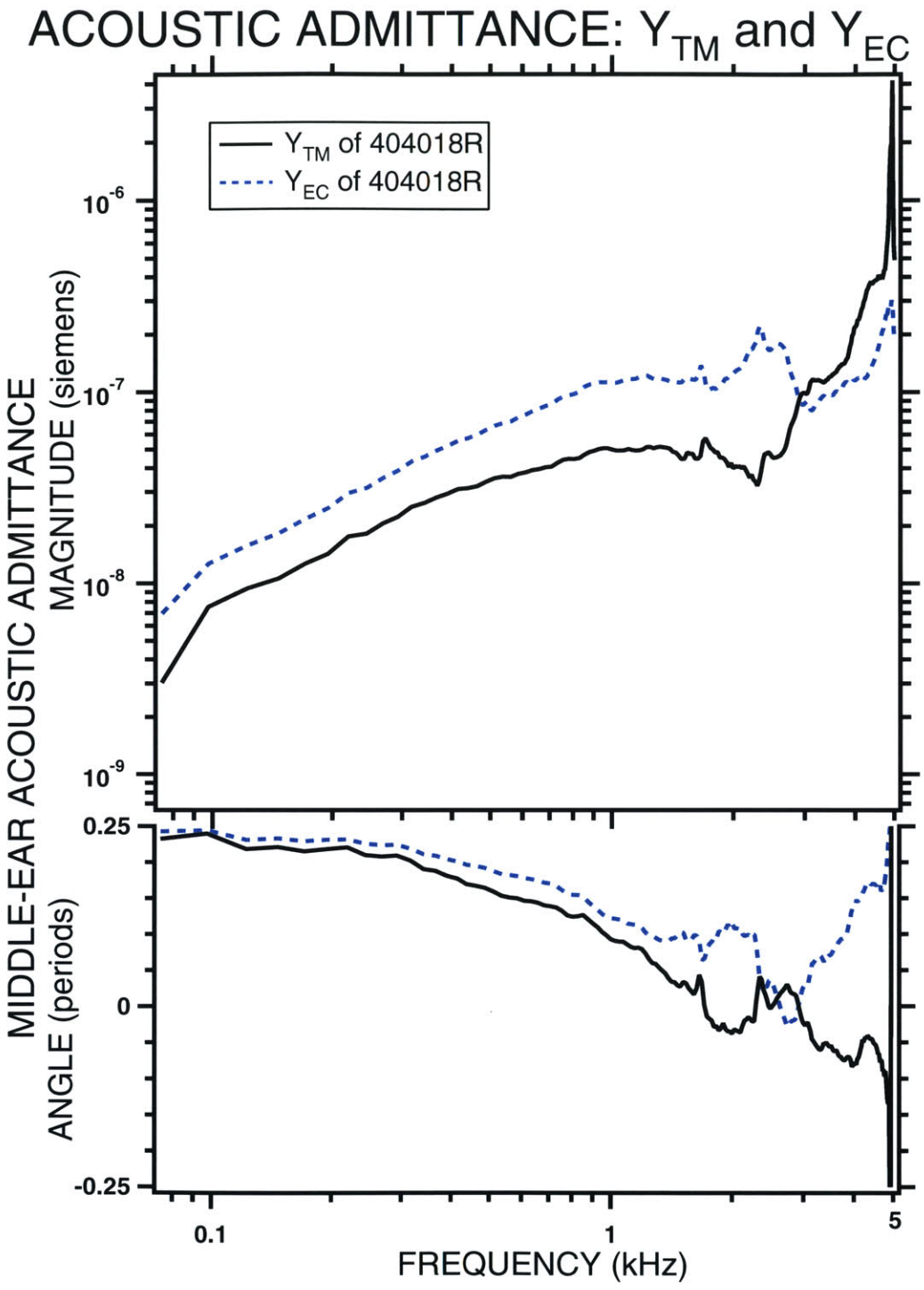

Figure 2.11: Y_{EC} and Y_{TM} of the right ear of 404018, a one-year old female sand cat. Y_{TM} is determined from Y_{EC} using a transformation modeled by a lossless uniform canal.

2.4.9 Statistical Analysis

Mean admittances magnitude of each species is determined by averaging of log magnitudes of individual ears. Mean admittance angles are determined by averaging the angles of individual ears. The frequency range of usable data varied due to the accuracy of load prediction. As a result, the number of ears included in an average varied with frequency, decreasing at higher frequencies.

The mean power absorption magnitude is determined by averaging the log magnitude the real part of the admittances of individual ears. In some ears, the real parts were negative (because the angle of the admittance is greater 0.25 periods) and these data were discarded. As a consequence, the number of ears averaged at each frequency varied between 17 and 19.

2.5 Auditory Brainstem Response (ABR)

The Auditory Brainstem responses (ABRs) were measured by the team from Boys Town National Research Hospital. ABRs can determine the sensitivity of the cat's hearing by measuring the electrical activity of the auditory system occurring within 10 ms following the onset of an acoustic stimulus.

2.5.1 Hardware

ABRs were measured by a separate computer that was connected to the SAME acoustic assembly, ER10C, used in the acoustic measurements to generate the stimulus. The computer amplified differentially the potential across two platinum sub dermal-needle electrodes (Grass Instruments).

2.5.2 Technique

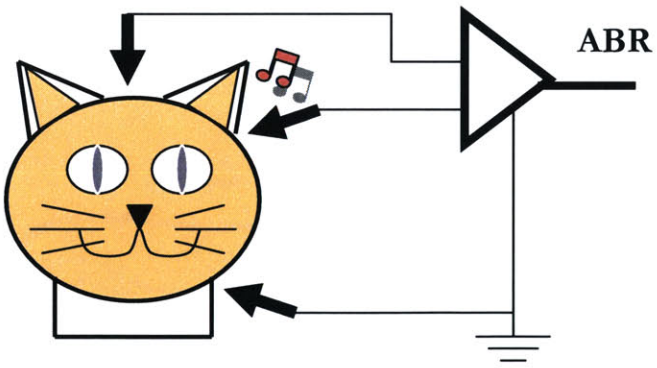

Figure 2.12: Cartoon of the setup for measuring auditory brainstem responses. Electrodes are places at the vertex of the head, behind the ear, and on the neck. The amplified electric potential difference between the vertex and the ear is the measured auditory brainstem response (ABR).

The electrodes were positioned as in Figure 2.12. Stimulus tone bursts were generated digitally at a sample rate of 192 kHz and delivered at approximately 21/sec. Tone bursts at 1 kHz and higher were 3ms duration (1 ms raised cosine on/off ramps and 1 ms plateau) and are presented in alternating phase. Tone bursts below 1 kHz are presented with 1 cycle on/off ramps (raised cosine) and a 1 cycle plateau for a total duration of 3 cycles where the phase was fixed.

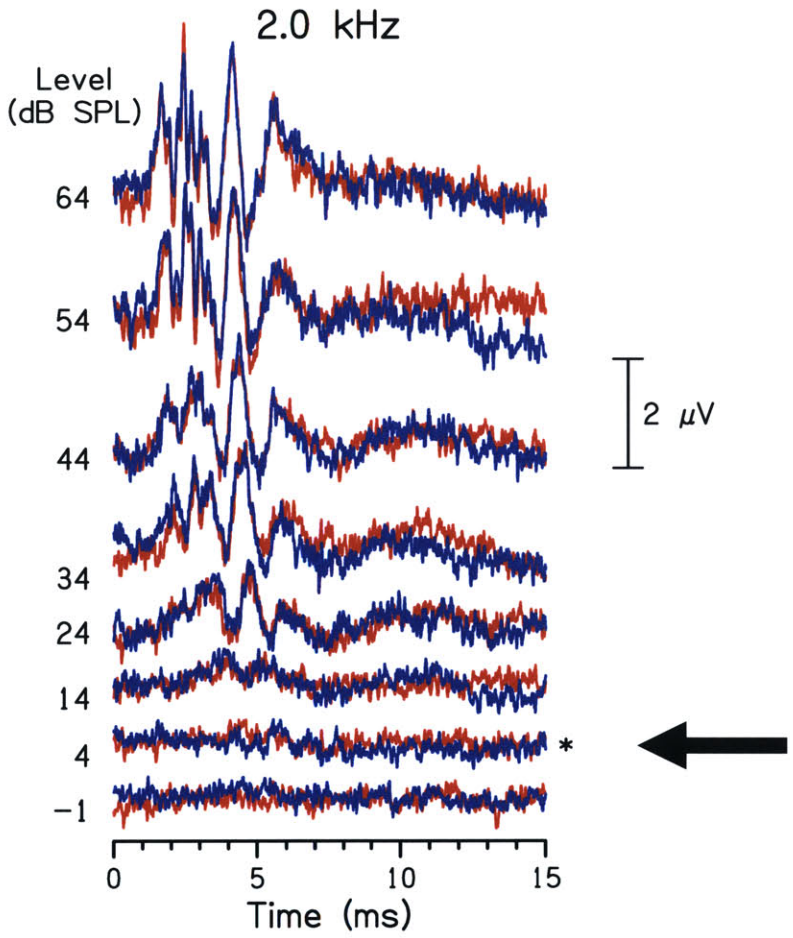

Figure 2.13: Time-varying auditory brainstem responses of 404018, a one-year old female sand cat, to tone bursts at 2 kHz with decreasing amplitude for each lower trace. The threshold value at this frequency was determined by the last perceivable response which is at 4 dB (from Walsh and McGee, unpublished). Two waveforms for identical stimuli are displayed (red and blue) for each stimulus level to allow judgment of the repeatability of a "response."

The potential differences between the vertex and ear were amplified 100,000X, band-pass filtered (0.03 - 10 kHz; Grass Model P511K), and digitized (Lynx L22, 24-bit soundcard) at a sampling rate of 192 kHz over a 15 ms epoch. Two repeated averaged waveforms, from vertex to ear electrodes, were obtained for each stimulus condition. (Trials with extraneously high voltages due to muscle artifact are automatically excluded from the average.) Upon completion of a run, response waveforms were stored digitally for off-line analyses. The ABR thresholds were then estimated subjectively by selecting the lowest stimulus level that produced replicable responses (Figure 2.13).

3 Results

3.1 Overview

In this section, we describe the measurements we obtained at The Living Desert. Table 3.1 is a summary of 8 measurements made on or inferred for all ears: (1) the ear(s) that were measured, (2) skull dimensions, (3) pinna area, (4) body mass, (5) large and (6) small diameter of the ear canal measured from the ear molds, (7) the calculated ear canal area, (8) inferred ear canal volume from low frequency acoustic measurement, and (9) inferred ear canal length from the eartip to the tympanic membrane. The mean body mass of the individual species range from the smallest to the largest in the following order: sand cat, Arabian wildcat, bobcat, caracal, and serval (Table 3.2). Sand cat had the largest average ear-canal cross-sectional area, while the serval had the largest pinna area. A total of 37 ears were examined at The Living Desert, however only 26 ears were used in the analysis. Some reasons for exclusion were ear-canal cross sectional areas, volumes, and lengths not consistent with the species means, dirty ear canals, and irregular behavior of the ear's tympanogram. Table 3.3 provides a summary of the number of individual ears from specimens used in the analysis. In the data collected, the number of Sand cats (19) is more than two times the number of all other specimens combined (8).

Table 3.1: Measurements Made at The Living Desert, July 2004

Species	Specimen	(1) Ear	(2) Skull Dimensions			(3) Pinna Area (cm^2)	(4) Mass (kg)	Diameters of the ear canal		(7) Ear Canal Cross-sectional Area, A_{EC} (mm^3)	(8) Inferred Ear Canal Volume (cc), V_{EC}	(9) Inferred ear canal length, L_{EC} V_{EC}/A_{EC} (mm)
			L_G (mm)	W_Z (mm)	W_P (mm)			(5) Larger Diameter, D_L (mm)	(6) Smaller Diameter, D_S (mm)			
Sand cat (*Felis margarita*)	Mukha	R	93	70	42	14.50	2.60	7.50	7.20	42.4	0.409	9.6
	Oasis	R	93	57	51	-	1.80	8.26	7.64	49.6	0.701	14.2
	Chaffa	R*	101	69	55	9.75	2.85	-	-	-	-	-
		L	-	-	-	-	-	7.62	7.56	45.2	1.170	25.9
	Persephone	R*	90	63	28	11.64	1.70	†7.60	†7.60	45.4	2.580	56.8
	404018	R	93	55	34	9.09	1.75	7.80	6.02	36.9	1.160	31.4
		L	-	-	-	-	-	8.18	7.10	45.6	0.763	16.7
	404015	R	97	73	33	13.69	2.65	8.32	7.20	47.0	0.652	13.9
	404020	R	89	68	30	9.70	1.80	8.22	6.60	42.6	1.165	27.3
	404016	R*	73	56	53	14.71	2.40	8.10	7.22	-	-	-
		L	-	-	-	-	-	8.12	7.70	49.1	0.498	10.1
	Naiade	R*	92	67	44	14.09	2.00	7.80	6.14	-	-	-
		L	-	-	-	-	-	7.80	6.72	41.2	0.720	17.5
	Lasmine	L*	98	61	32	12.27	2.45	-	-	-	-	-
	Bart	R*	90	67	40	12.66	2.30	-	-	-	-	-
		L	-	-	-	-	-	†7.60	†7.60	45.4	0.496	10.9
	Millhouse	R	103	73	39	14.24	-	†7.60	†7.60	45.4	0.791	17.4
	404024	R	84	61	38	15.65	2.05	†7.60	†7.60	45.4	0.633	14.0
	404014	R	84	68	34	11.66	2.05	8.52	7.46	49.9	0.604	12.1
		L*	-	-	-	-	-	8.22	6.58	-	-	-
	404013	R	97	72	36	15.94	2.35	7.38	7.30	43.0	0.875	20.3
		L	-	-	-	13.58	-	†7.60	†7.60	45.4	0.704	15.5
	404017	R	-	-	-	-	1.95	7.90	7.04	43.7	0.406	9.3
		L	-	-	-	-	-	8.12	7.26	46.3	0.693	15.0
	404019	R	-	-	-	-	1.75	8.20	7.74	49.8	0.899	18.0
Arabian Wildcat	Lance	R	93	71	41	12.32	4.25	6.68	5.82	30.5	1.042	34.1
		L	-	-	-	12.31	-	7.36	5.70	32.9	1.240	3 7.6

(Felis silvestris)	Rip	R*	94	62	33	11.37	-	7.12	5.60	-	-	-
		L*	-	-	-	-	-	-	-	32.3	0.175	5.4
Serval ***(Leptailurus serval)***	Ruka	R	127	82	35	19.78	10.90	8.02	6.22	39.1	0.133	3.4
	Elijah	R	-	-	-	-	13.10	†6.40	†6.40	32.1	0.296	9.2
		L	-	-	-	-	-	†6.40	†6.40	32.1	0.151	4.7
Bobcat ***(Lynx rufus)***	Reebok	R	150	95	45	16.50	11.10	†6.20	†6.20	30.2	1.020	33.7
	Crawler	R	126	82	31	13.51	9.10	†6.20	†6.20	30.2	0.602	19.9
	Nike	R*	-	-	-	-	9.10	6.94	6.68	-	-	-
Caracal ***(Caracal caracal)***	Tippy	R	-	-	-	-	10.75	†6.40	†6.40	32.2	0.258	8.0
Ocelot	Brazil	L*	-	-	-	-	10.70	-	-	-	-	-

(1) R denotes right ear. L denotes left ear.

* Denotes an ear not used in the analysis. Reasons for exclusion include ear-canal cross-sectional areas, volumes, and lengths from eartip to the TM that are not consistent with species means as well as tympanograms with irregular responses to static pressure change.

(2) L_G = Greatest length from top of upper incisors to nuchal ridge. W_Z = Largest width at zygoma. W_P = Greatest width of mastoids.

(3) The area of the pinna was calculated using Heron's formula.

(4) and (5) The diameters of a specimens' ear canal were measured from ear molds.

† In some specimens, ear-mold material was not injected deep enough into the ear to capture the dimensions of the ear canal. In sand cat specimens where diameters could not be measured from the ear molds, the mean squared radius ($D_L/2 * D_S/2$) from the other sand cat ears was used to calculated the cross-sectional area. In serval, bobcat, and caracal specimens, radius, used in the calculation of the cross-sectional ear canal area, is determined from bony-ear-canal dimensions obtained from skull museum measurements multiplied by a conversion factor to account for the difference in diameters between the bony and cartilaginous ear canals. As a conversion factor we used the ratio of the average sand cat cartilaginous ear canal radius to the average sand cat bony ear canal measurements from skulls.

(6) Cross-sectional Area of the ear canal is calculated from the two diameters using the equation, $A_{EC} = \pi * D_L/2 * D_S/2$.

(7) Inferred ear canal volume is determined from the acoustic compliance value extracted from the tympanogram at the most negative static pressure.

(8) Inferred length from eartip to the TM, $L_{EC} = V_{EC}/A_{EC}$.

(-) No Measurements obtained.

Table 3.2: Species Means

Species	Mean Mass ±SEM	Mean Ear-canal Cross-sectional Area ±SEM	Mean Pinna Area ±SEM
Sand cat (***Felis margarita***)	2.153±0.091 (N=16)	45.217±0.786 (N=18)	12.878±0.557 (N=16)
Serval (***Leptailurus serval***)	12±1.100 (N=2)	34.433±2.333 (N=3)	19.78 (N=1)
Bobcat (***Lynx rufus***)	9.767±0.667 (N=3)	30.2 (N=2)	15.005±1.495 (N=2)
Arabian Wildcat (***Felis silvestris***)	4.25 (N=1)	31.7±1.200 (N=2)	12±0.315 (N=3)
Caracal (**Caracal caracal**)	10.75 (N=1)	32.2 (N=1)	-

Table 3.3: Summary of the Ears Measured and Used for Analysis

Species	Specimens	Ears Measured	Ears with acoustic data	Ears with ABR data	Ears with Both data set
Sand cat	16	25	18	16	16
Serval	2	3	3	2	2
Bobcat	3	3	2	3	2
Arabian wildcat	2	4	2	1	1
Caracal	1	1	1	1	1
Ocelot	1	1	0	0	0

3.2 Acoustic Measurements

3.2.1 Overview

In this section, the measurements of acoustic input-admittance are reported first as individual ears, then across species, and finally as sand cat versus the non-sand cat group. Then, the average power absorption of ears in each of the five felid species is reported. Figure 3.1 shows the admittance of 19 individual sand cat ears. Figure 3.2 shows the

admittance of 3 serval ears and 1 caracal ear. Figure 3.3 shows the admittance of 2 bobcat ears and 2 Arabian wildcat ears. Figure 3.4 shows the means of the acoustic input admittances for the five species. Figure 3.5 plots the means of the input-acoustic admittance of sand cats and non-sand cats with statistically significant difference indicated on the plot. Figure 3.6 shows the means of the power absorption at the tympanic membrane for the five species. Figure 3.7 plots the means of the power absorption between sand cats and non-sand cats, with statistically significant differences indicated. The plotted results are discussed separately for low and high frequency regions.

3.2.2 Acoustic Input Admittance

3.2.2.1 Individual Sand cats (Figure 3.1)

Low Frequency (0.075 – 0.8 kHz)

Magnitude

The admittance magnitudes of the individual sand cat ears have similar features and are clustered generally within a span of a factor of 2. The $|Y_{TM}|$ generally are proportional to frequency and a constant slope close to 1 in the log-log plot of Figure 3.1. Three ears have been singled out in the plot because these ears have unusual admittance feature despite not having unusual ear canal cross-sectional areas, or volume and the behavior of

their tympanograms satisfy all 3 acceptance criteria (see Methods). The left ear of 404013, a noticeable outlier in magnitude, has a $|Y_{TM}|$ that is a factor of 2.5 below the rest of the sand cat group in this frequency range.

Angle

Nearly all ear angles of the Y_{TM} are close to 0.25 periods up to 0.3 kHz and then decrease.

High Frequency (0.8 – 5 kHz)

Magnitude

The frequency dependence of the admittance magnitudes the individual sand cat ears have more complex frequency dependence in this frequency range and span about a factor of 3 at any frequency. The left ear of Chaffa and the right ear of 404018 have a peak and valley close to 5 kHz, in which $|Y_{TM}|$ spans more than a factor of 10; this features are not seen in the other sand cat $|Y_{TM}|$'s.

Angle

Near 2 kHz, most angles are around 0 degrees. ChaffaL and 404018R have angles that change sharply between 90 and -90 degrees at the frequency of the sharp dip (ChaffaL) or peak (404018R) in $|Y_{TM}|$.

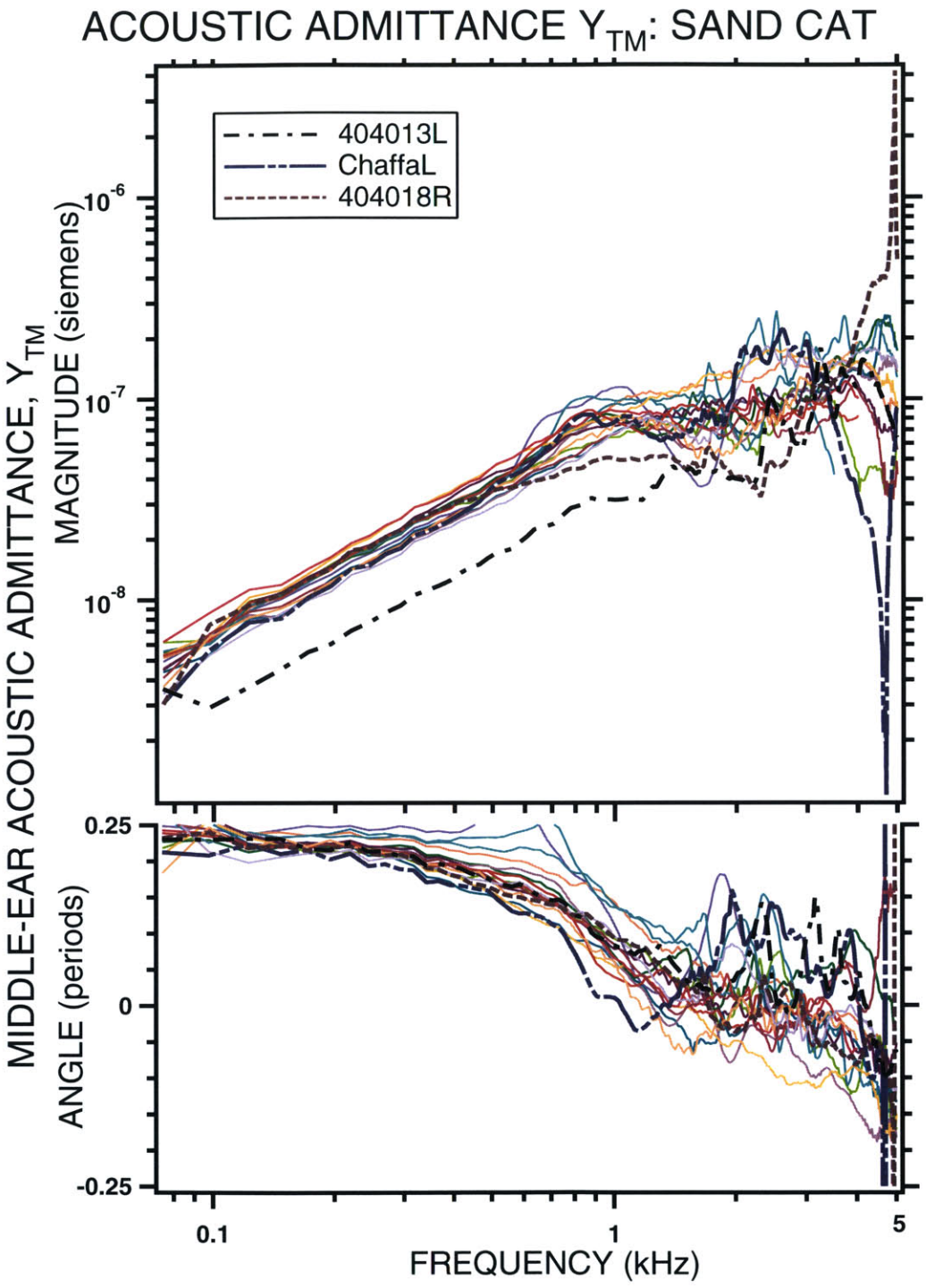

Figure 3.1: Acoustic Input Admittance of Individual Sand cat ears. There are admittance measurements from 18 ears of 16 sand cats. Admittance values are plotted for the frequency range in which measured loads do not have large errors. Four individual ears are distinguished because they have unusual features compare to the rest of the group.

3.2.2.2 Individual Servals (Figure 3.2)

Low frequency (0.075 – 0.8 kHz)

Magnitude

The admittance magnitudes of the 3 serval ears have similar feature. All three serval $|Y_{TM}|$s are proportional to frequency up to 0.4 kHz; the group spans a factor of 1.4 in $|Y_{TM}|$. All three reach local maxima between 0.5 and 1.1 kHz.

Angle

Angles for these serval ears are around 0.2 periods up to 0.5 kHz. All three angles of serval ears drop suddenly to below 0 periods at around the frequency where their respective $|Y_{TM}|$ reaches its maximum.

High Frequency (0.8 – 5 kHz)

Magnitude

The magnitude of all three individual serval ears has a large drop in magnitude to reach a local minimum at different frequencies and all three ears increase in magnitude after the local minimum.

Angle

The angles for all three servals changed from 0.2 periods to -0.2 periods, where the steep drop starts between 0.5 kHz to 1.2 kHz. Then, all three ears have sharp increases in angle, to a maximum of about 0.10 periods, at the frequency where their respective magnitude minimum occurs.

3.2.2.3 Individual Caracal (Figure 3.2)

Low frequency (0.075 – 0.8 kHz)

Magnitude

The admittance magnitude of caracal is proportional to frequency up to 0.7 kHz. At 0.9 kHz, the magnitude reached its first local maximum.

Angle

The admittance angle has a sharp drop from 0.1 periods to -0.15 periods starting at 0.8 kHz, i.e. around the local maximum in magnitude.

High Frequency (0.8 – 5 kHz)

Magnitude

The admittance magnitude of the caracal remains fairly constant in much of this frequency range. At 4.5 kHz, $|Y_{TM}|$ reaches its second maximum.

Angle

The angle of the caracal admittance is roughly constant between -0.15 and -0.2 periods within this frequency range.

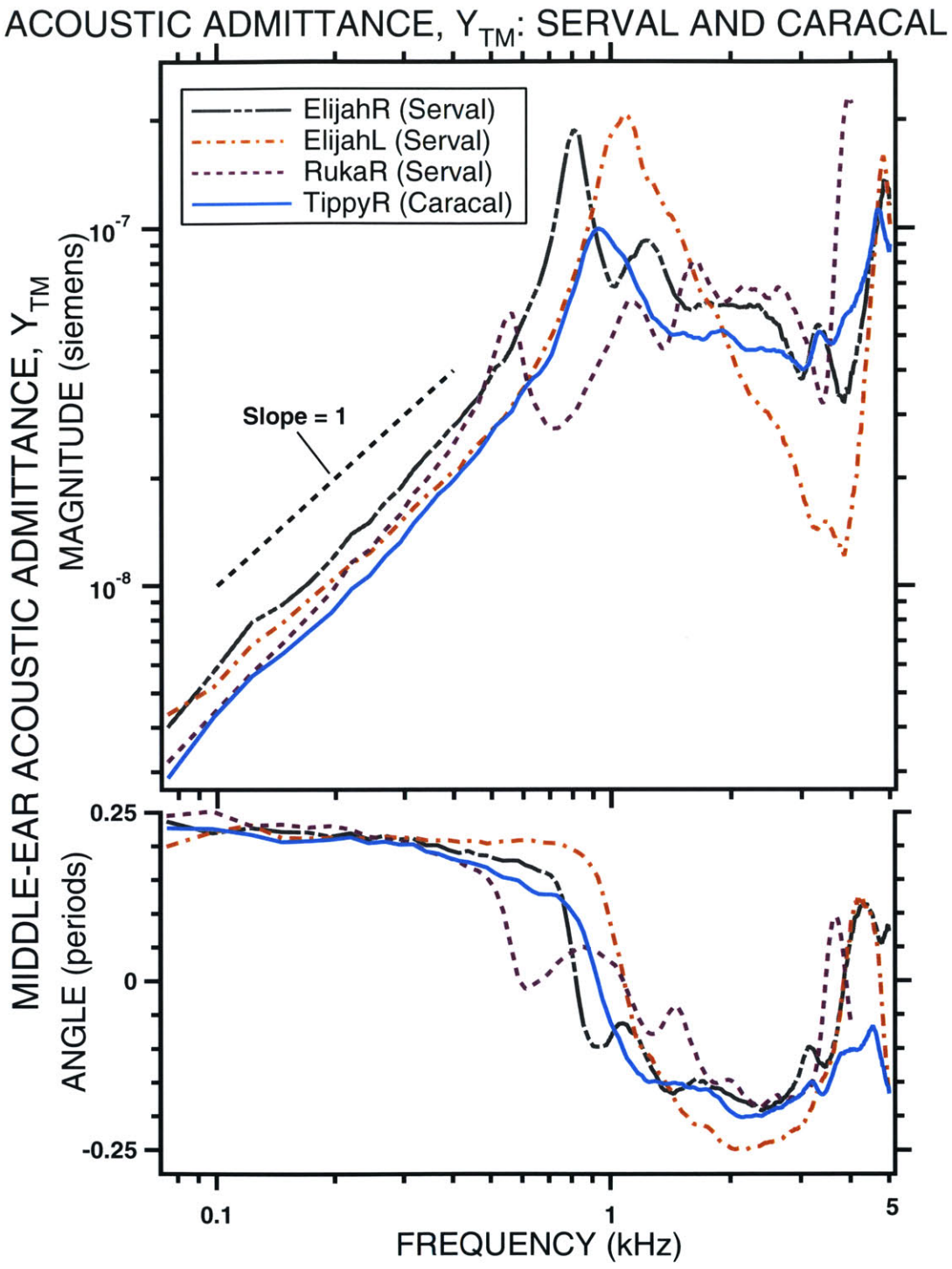

Figure 3.2: Measured acoustic input admittance of 3 serval ears and 1 caracal ear.

3.2.2.4 Individual Bobcats (Figure 3.3)

Low frequency (0.075 – 0.8 kHz)

Magnitude

The admittance magnitudes of the individual bobcat ears have similar features. Both $|Y_{TM}|$s are roughly proportional to frequency up to 0.5 kHz.

Angle

Both angles decrease roughly linearly from 0.25 periods to -0.05 periods with frequency between 0.075 kHz to 0.8 kHz.

High Frequency (0.8 – 5 kHz)

Magnitude

The $|Y_{TM}|$ of Crawler's right ear is fairly constant while Reebok's $|Y_{TM}|$ increases between 4 – 5 kHz. The admittance magnitude of Reebok's right ear reaches a sharp local minimum at 4 kHz.

Angle

The angles of both bobcat ears increase from 2 – 3 kHz with roughly a 0.10 period difference between ears.

3.2.2.5 Individual Arabian wildcats (Figure 3.3)

Low frequency (0.075 – 0.8 kHz)

Magnitude

The admittance magnitude of the both Arabian wildcat's ears increase linearly with frequency; they differ at most by a factor of 3.

Angle

Both angles decrease linearly from 0.25 periods to -0.05 periods with frequency between 0.075 kHz to 0.8 kHz.

High Frequency (0.8 – 5 kHz)

Magnitude

The admittance magnitudes of the two Arabian wildcat do not behave similarly. The left ear of Lance reaches a maximum at 3 kHz, whereas the right ear reaches a maximum at 5 kHz.

Angle

The admittance angles also do not behave similarly. For the right, it is roughly constant around ±0.20 periods between 2 kHz to 4 kHz, while angles for left of Lance are roughly constant at -0.10 periods in the high frequency range.

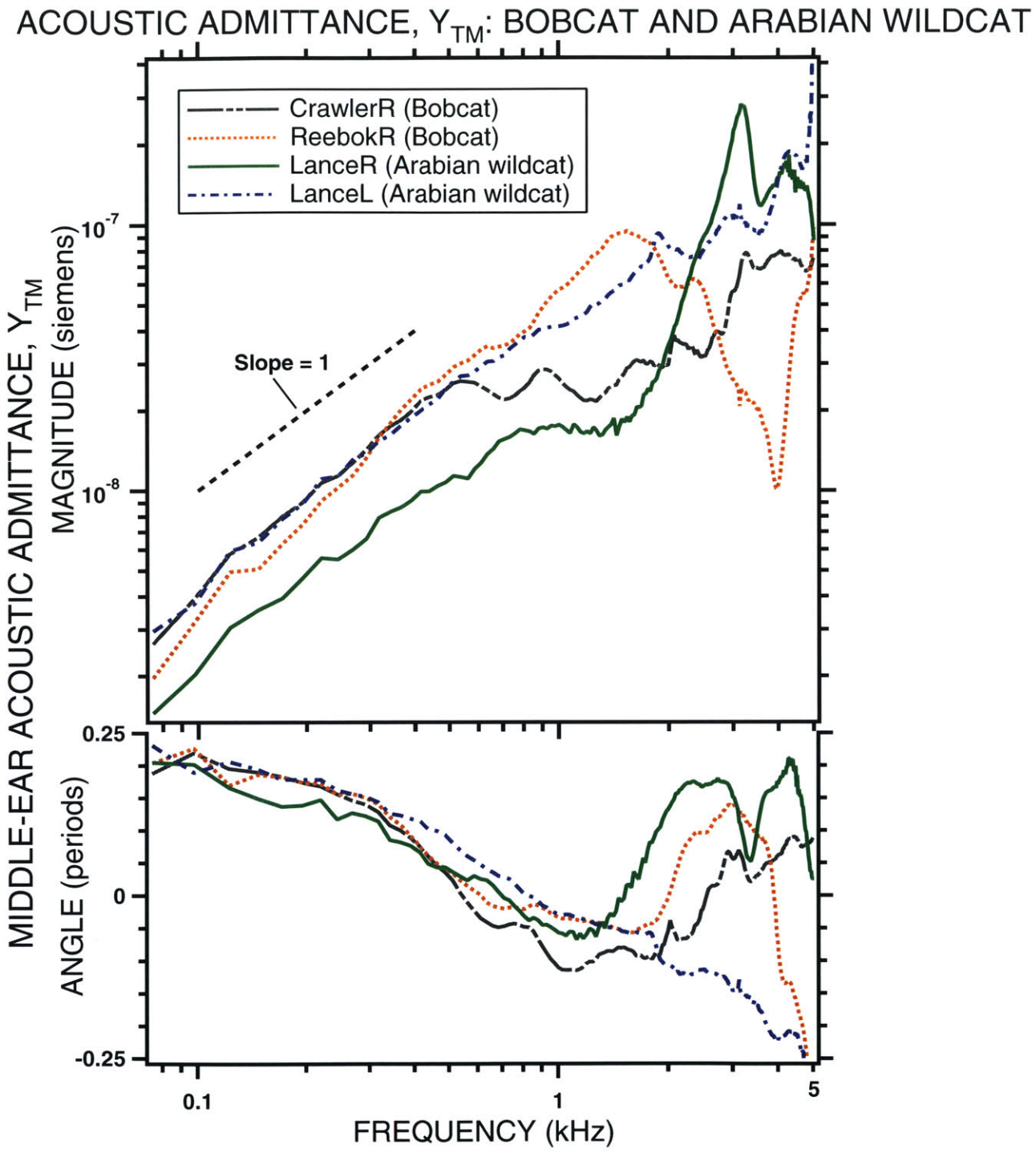

Figure 3.3: Acoustic Input Admittance measurements from 2 bobcat and 2 Arabian wildcat ears.

3.2.2.6 Species Means (Figure 3.4)

Low frequency (0.075 – 0.8 kHz)

Magnitude

At frequencies between 0.075 kHz and 0.8 kHz, the middle ear acoustic input admittances (Y_{TM}) have qualitatively similar feature across the five species. The magnitude of the input acoustic-admittance is roughly proportional to frequency with a slope of 1 on this log-log plot. Sand cats have the highest mean magnitude for frequencies less than 0.5 kHz.

Angle

At the lowest frequencies, the angle is close to 0.25 periods, which implies that the volume velocity of the TM, U_{TM}, leads the sound pressure at the TM, P_{TM} by 0.25 periods. Another way to describe this behavior is that the volume displacement is in-phrase with sound pressure in this frequency range. The motion of tympanic membrane at low frequencies can be characterized as controlled by elastic or compliant forces. For sand cats, bobcats, and caracal, the mean admittance angles remain above 0.2 periods up to 700 Hz. For servals and the Arabian wildcat, the admittance angles are smaller and decrease at a steeper slope from 75Hz to 850 Hz. At 800 Hz, the angles are near 0 for serval and the wildcat, implying that the admittances are resistance-like.

High Frequency (0.8 – 4 kHz)

Magnitude

Between frequencies of 850Hz and 4000Hz, the admittance magnitude across species can be described as having no clear trend (up or down) over the whole range; although $|Y_{TM}|$ changes little over the range, each has sizable ups and downs. The magnitude of sand cats increases but at a slower rate than at low frequencies. In the same frequency range, the $|Y_{TM}|$ of servals and caracal have a minimum, which may result from the coupling of middle-ear cavities (Huang, et al 2000, p. 463). The absence of such a sharp minimum in the sand-cat results is consistent with the summary of similar measurement (Huang, et al. 2002, Fig 463). The Arabian wildcat measurement also lacks a well-defined minimum in $|Y_{TM}|$ but has a prominent sharp peak at 3 kHz.

Angle

Between frequencies of 0.8 kHz and 4 kHz, only the sand cat results remain approximately resistive (i.e. angle $\approx$ 0) to the upper end of the frequency range. The angles for the bobcat and the caracal change steeply from +0.2 periods to -0.2 periods at the range of 0.5 kHz to 2 kHz, where servals and Arabian wildcat angle slopes less steeply and returns to positive values for frequencies greater than 2 kHz.

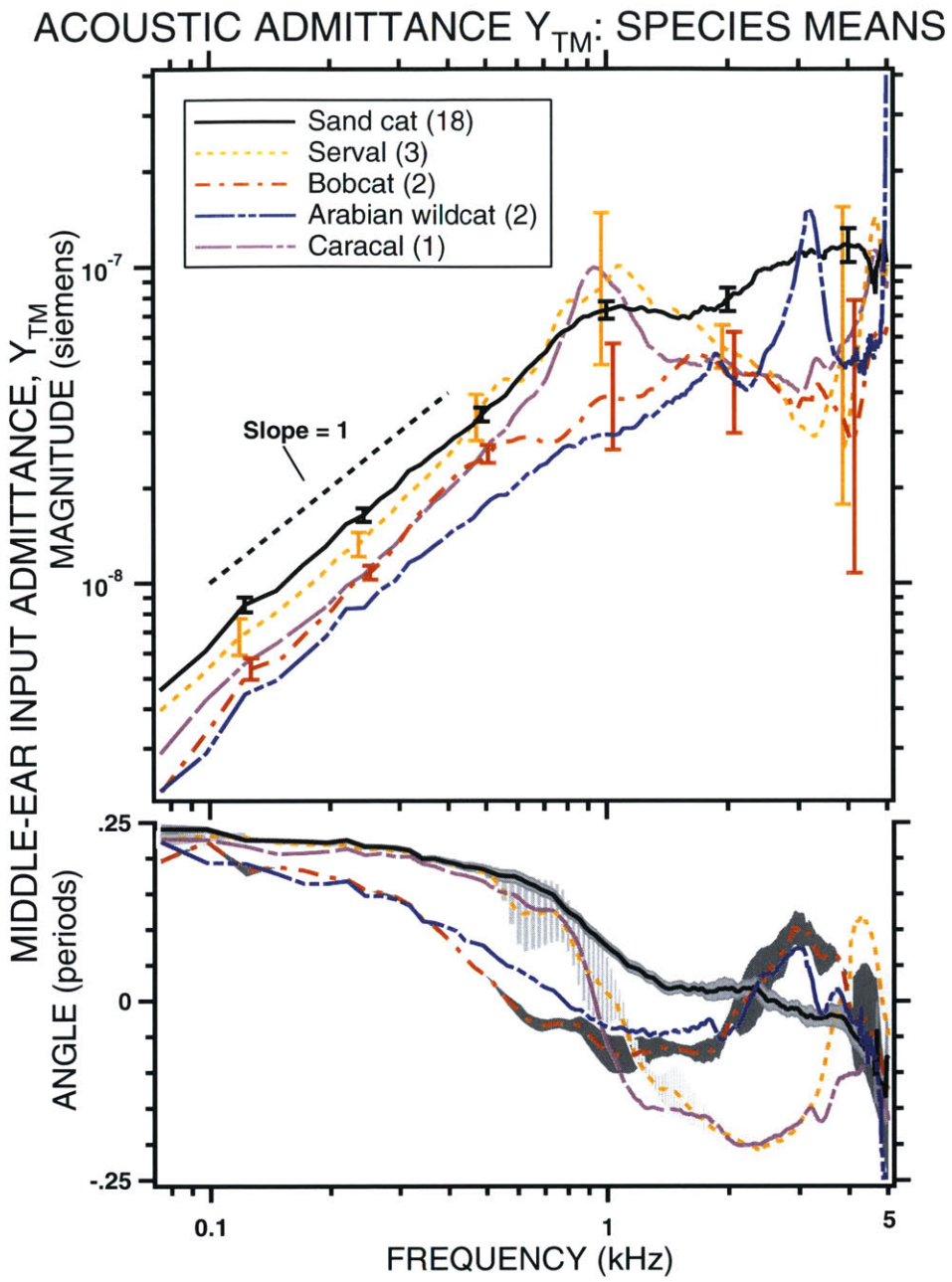

Figure 3.4: Means of middle-ear admittance measurement at the tympanic membrane (Y_{TM}) for sample of five felid species. Upper: Magnitude means. Lower: Angle means. Only ears with both acoustic and ABR data are plotted. For each ear, Y_{TM} is calculated with a transformation from Y_{EC} using the measured canal area, A_{EC}, and the inferred length, L_{EC}, of the distance between the eartip and the tympanic membrane. Y_{TM} of each ear, even those from the same animal, is calculated separately; for each species, log Y_{TM} magnitude and angle are averaged across ears. The vertical bars on the magnitude graph span mean ± SEM. The bars occur at 0.125, 0.25, 0.5, 1, 2, and 4 kHz, which include the frequencies at which ABR threshold values were determined. In the angle plot, the ±one-standard-error range about the mean is shaded over the entire frequency range. In the magnitude plot, the admittance curves for serval and bobcats have been shifted horizontally by ±40 Hz in order to separate the vertical error bars.

3.2.2.7 Statistical Differences: Admittance, Y_{TM} of Sand cat vs. Non-sand cat (Figure 3.5)

We are interested in whether sand cats' ears are acoustically specialized compare to other felid species; to do statistical tests (with enlarged sample size), we divided the ears into two groups: sand cats (N=16) and non-sand cats (N=6). We test for statistical differences at frequencies of 0.125, 0.25, 0.5, 1, 2, and 4 kHz. These frequencies were chosen to correspond to the data available for the threshold of the auditory brainstem responses (with the exception of the 0.125 kHz, which was only tested in the acoustic data). The mean acoustic admittance magnitude of sand cats is significantly different from that of non-sand cats at 0.125, 0.25, 0.5, 2 kHz (see Table 3.4). The mean acoustic admittance angle of sand cats is significantly different from that of non-sand cats at 0.25, 0.5, 1, 2 kHz. The means at 1 and 4 kHz differ by as much or more than those at other frequencies, but the SEMs are larger for the non-sand cat groups, which is important in determining significance. The angles at 0.125 kHz are very close to being significantly different. Thus, the difference in angle between the two groups seems to occur at low frequencies.

Table 3.4: Statistical Difference for Y_{TM}: Sand cat vs. Non-sand cat

	Magnitude			Angle		
Frequency (kHz)	Statistical Difference (95% confidence)	T Stat	P(T<=t) two tail	Statistical Difference (95% confidence)	t Stat	P(T<=t) two tail
0.125	Y	4.869	0.0002	N	2.151	0.0637
0.25	Y	4.762	0.0003	Y	2.886	0.0203
0.5	Y	2.412	0.0345	Y	2.718	0.0263
1	N	0.455	0.6611	Y	4.679	0.0011
2	Y	3.234	0.0037	Y	2.568	0.0303
4	N	1.298	0.2234	N	-0.545	0.5988

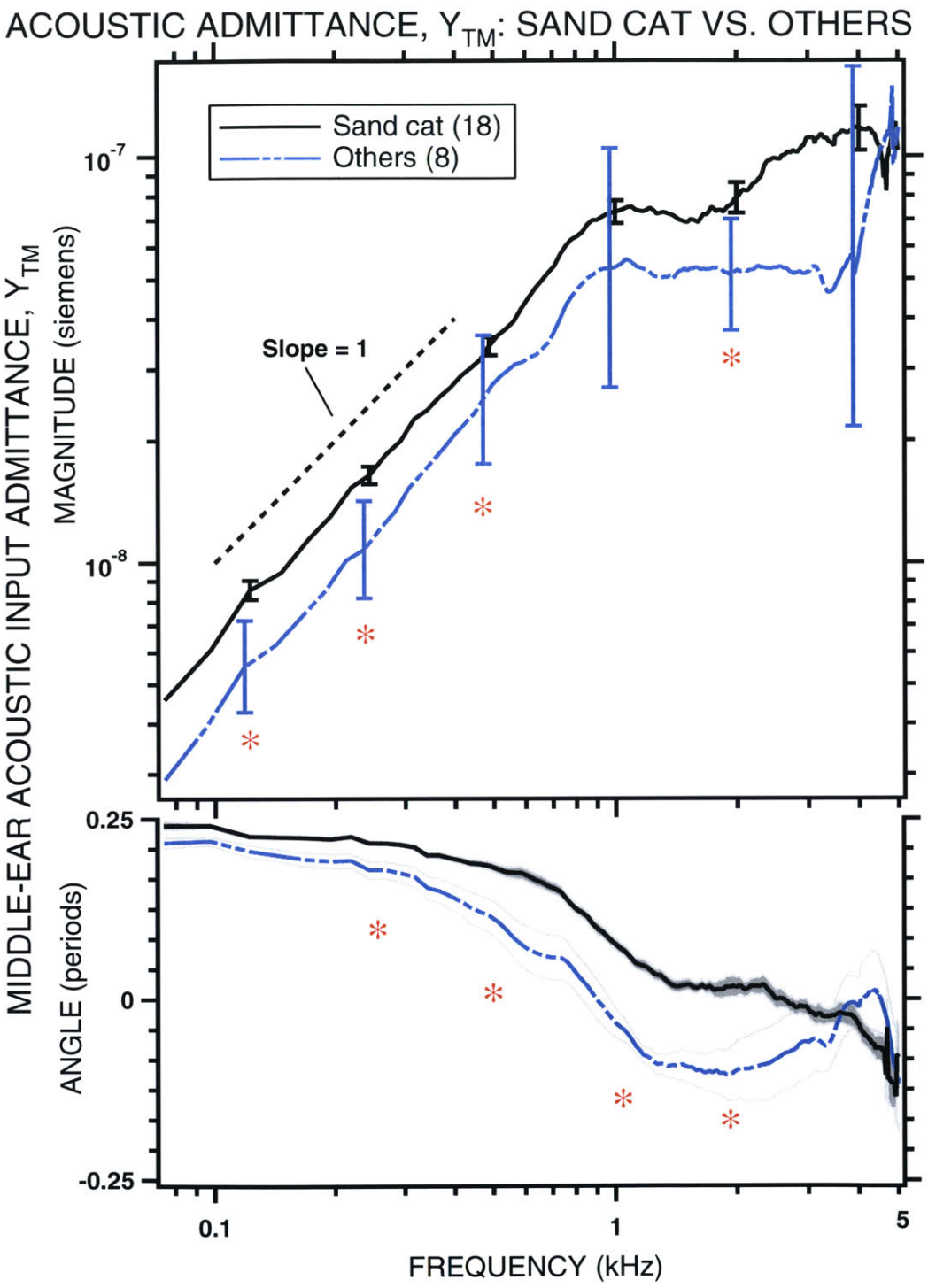

Figure 3.5: Means of the admittance at the tympanic membrane (Y_{TM}) for ear of sand cat and non-sand cats. The non-sand-cat group is made up of 2 servals, 2 bobcats, a caracal, and an Arabian wildcat. The vertical bars in the upper graph indicate ± one standard error away from the mean. The bars occur at 0.125, 0.25, 0.5, 1, 2, and 4 kHz. In the angle plot, ± one-standard-error range from the mean is shaded for all frequencies. The curve of the non-sand cat group has been shifted downwards by 40Hz in order to distinguish the ±SEM. Asterisks denote a statistical difference with a 95% confidence level.

3.2.3 Power Absorption (Figure 3.6)

3.2.3.1 Magnitude

Low Frequency (0.075 – 0.8 kHz)

At frequency between 0.075 kHz and 0.8 kHz, the means of the real part of the Y_{TM} have similar features across species. The power absorption curves all have linear slopes close to 3 on a log-log scale. The servals and the Arabian wildcat have higher mean magnitude than those of the sand cats, bobcats, and caracal between 0.1 and 0.6 kHz.

High Frequency (0.8 – 4 kHz)

At frequency higher than 0.8 kHz, some of the power absorption curves are quite varied. The mean magnitude for the sand cats continues to increase albeit at a slower rate. Both the caracal and the bobcats have a large minimum 2 kHz and then continue climbing at around a slope of 2. The mean magnitude for the Arabian wildcat has a large maximum at 3 kHz.

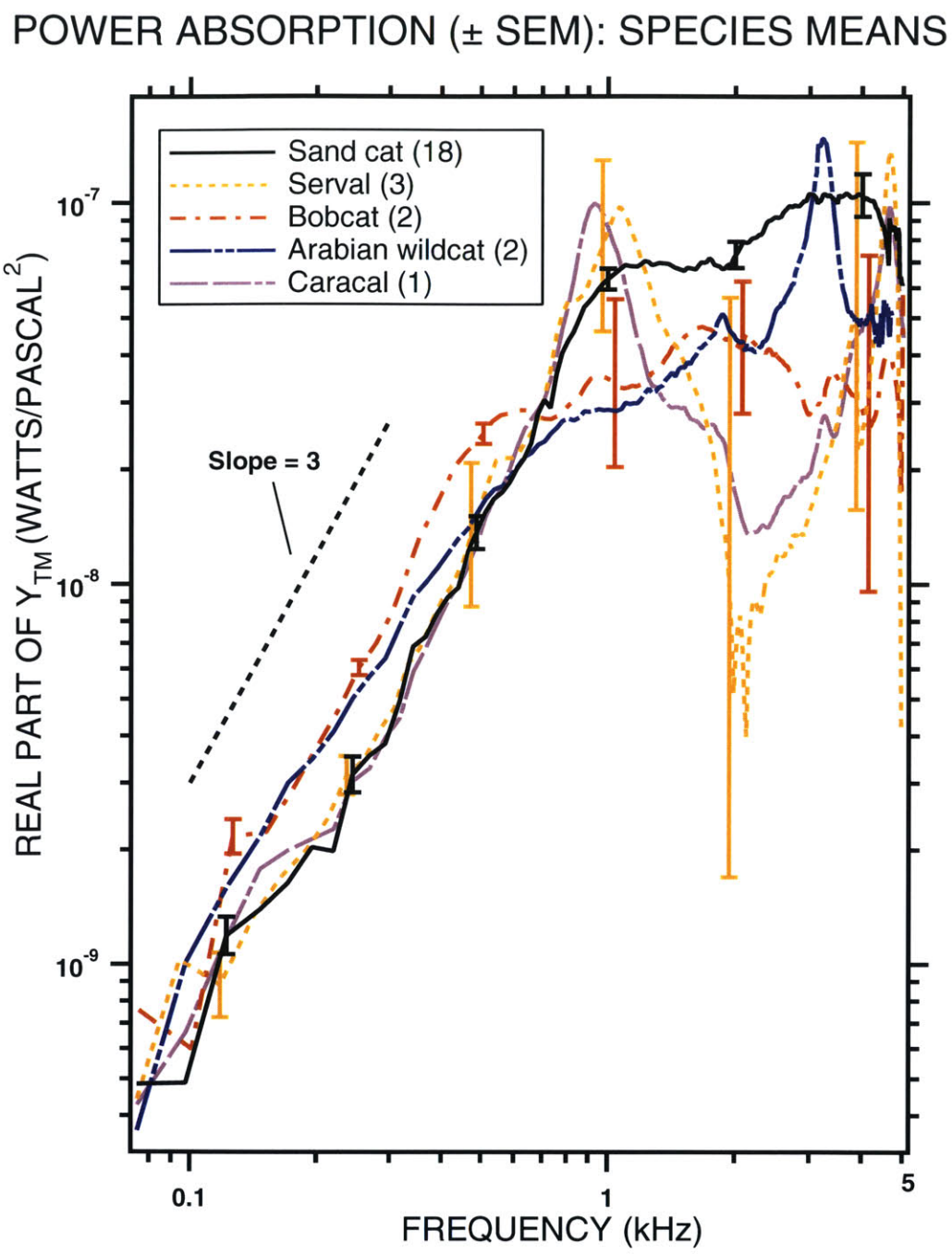

Figure 3.6: Means of the real part of the Y_{TM}s for five species. The real part of the magnitude of Y_{TM} is proportional to the average acoustic power absorbed at the tympanic membrane for a given sound pressure. The vertical bars on the plot indicate ± one standard error away from the mean and occur at 0.125, 0.25, 0.5, 1, 2, and 4 kHz. The power absorption curves for serval and bobcats have been shifted horizontally by ±40 Hz in order to distinguish ±SEM.

3.2.3.2 Statistical Differences: Sand Cat vs. Non-Sand Cat (Figure 3.7)

Overall, at frequencies below 1 kHz, the mean power absorption at the sand cat and the non-sand cat groups are statistically inextinguishable (Table 3.5). Both mean magnitude increase with a linear slope of 3 on the log-log scale for low frequencies(Figure 3.7). The mean power absorption between the two groups are significantly different at 2 and 4 kHz, where the mean differ much more at high frequencies than at low frequencies.

Table 3.5: Statistical Difference for Power Absorption: Sand cat vs. Non-sand cat

Frequency (kHz)	Statistical Difference (95% confidence)	t Stat	P(T<=t) two tail
0.125	N	-0.417	0.6833
0.25	N	-1.519	0.1570
0.5	N	-0.956	0.3616
1	N	0.281	0.7856
2	Y	4.514	0.0004
4	Y	2.209	0.0493

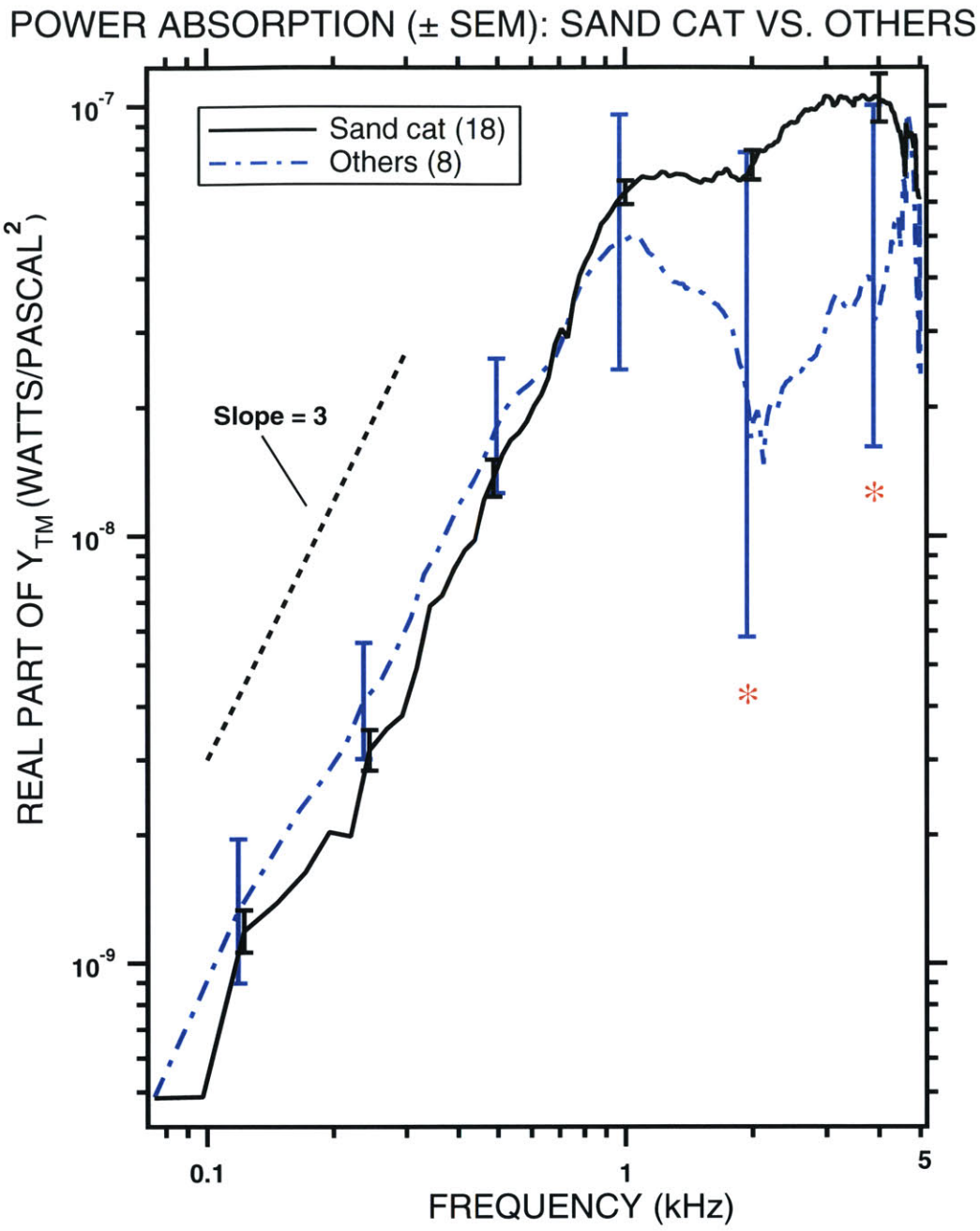

Figure 3.7: Means of the real part of the magnitude of Y_{TM} for the sand cat and non-sand cat group. The vertical bars on the plot indicate ± one standard error away from the mean. The bars occur at 0.125, 0.25, 0.5, 1, 2, and 4 kHz corresponding to the frequencies at which threshold values were determined. The power absorption curve for the non-sand cat group has been shifted down horizontally by 40 Hz in order to distinguish ±SEM. An asterisk denotes a statistical difference with a 95% confidence level.

3.3 Threshold of Auditory Brainstem Responses

3.3.1 Overview (Figure 3.8)

In this section, the threshold values determined by the auditory brainstem responses are reported for the discrete tone-burst frequencies, 0.25, 0.5, 1, 2, and 4 kHz. These frequencies are octaves apart starting at 0.25 Hz. Figure 3.8 plots the mean threshold obtained for five species. Figure 3.9 shows the threshold between sand cats and non-sand cats, where statistical significance are shown.

Low Frequency (0.25 – 1 kHz)

Between the frequencies of 0.25 kHz and 1 kHz, the threshold curves of four of the five species (with the exception of the caracal measurement) have similar features. Threshold decreases as the frequency increases within this range. At frequency below 1 kHz, the mean threshold of sand cats is the lowest. The sand cat threshold is lowest between 0.25 – 1 kHz but 1 Arabian wildcat threshold is close.

High Frequency (>1 kHz)

At frequencies above 1 kHz, it becomes harder to characterize the threshold curves across all species. The threshold values for the sand cat, bobcat, and Arabian wildcat continue to decrease and reach their lowest values at 2 kHz. Afterwards, the threshold value increases. For servals and caracal, there is noticeable increase in threshold values at 2 kHz before decreasing at 4 kHz.

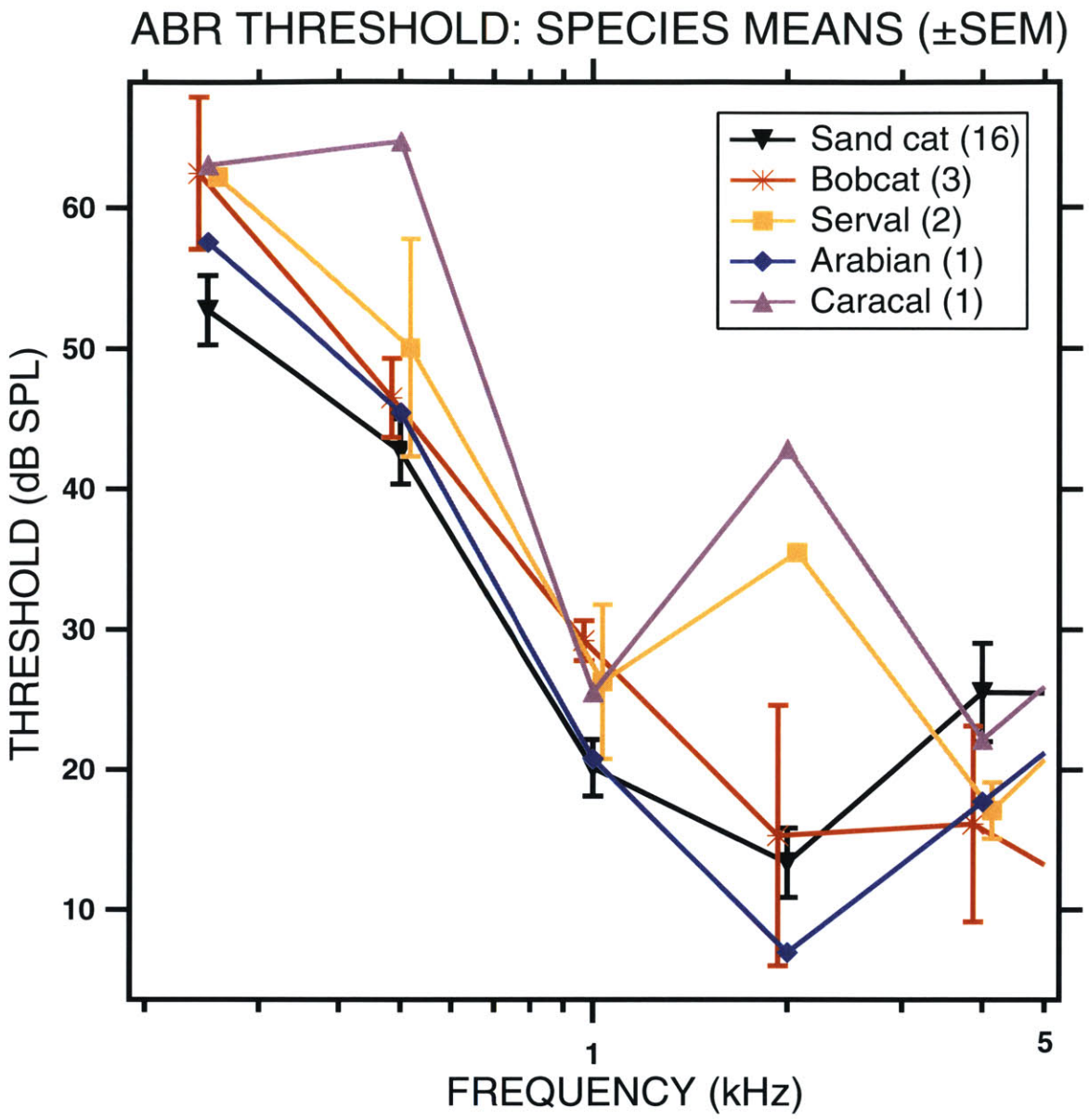

Figure 3.8: Threshold means determined from auditory brainstem responses across species. A specimen is given tone bursts stimulus of a specific frequency in the ear canal. Electric responses on the auditory nerve are recorded. The amplitude of the stimulus is decreased until no electrical responses can be visual detected. Thresholds were estimated as the lowest level of response on the auditory nerve (Figure 2.13). Threshold values for each specimen are determined at discrete frequencies an octave apart: 0.25, 0.5, 1, 2, and 4 kHz. The vertical bars on the magnitude graph span mean ± SEM. For Arabian and Caracal (N=1), no estimate of variability is shown. The threshold curves for servals and bobcats were shifted ±50 Hz in order to distinguish the ±SEM.

3.3.2 Statistical Difference: Sand Cat vs. Non-Sand Cat (Figure 3.9)

Because we are interested in how sand cats compare to non-sand cat species, we averaged the threshold values for all sand cats and for all the non-sand cat species. The contrast between the threshold curves is more apparent in this grouping. The mean thresholds of sand cat are lower than the non-sand cat grouping and for all frequencies of 2 kHz and below (Figure 3.9). At 4 kHz, the sand cat threshold values go above the non-sand cat threshold means. Mean sand cat thresholds are statistically significant lower at both 0.25 kHz and at 1 kHz than the other group (Table 3.6) and marginal at 0.5 kHz and 4 kHz.

Table 3.6: Statistical Difference for ABR Threshold: Sand Cat vs. Non-sand cat

Frequency (kHz)	Difference of Means	Statistically Different (95% confidence)	t Stat	P(T<=t) two tail
0.25	9.27	Y	-2.946	0.008
0.5	7.25	N	-1.843	0.088
1	6.51	Y	-2.460	0.024
2	10.44	N	-1.621	0.144
4	-8.06	N	1.910	0.070

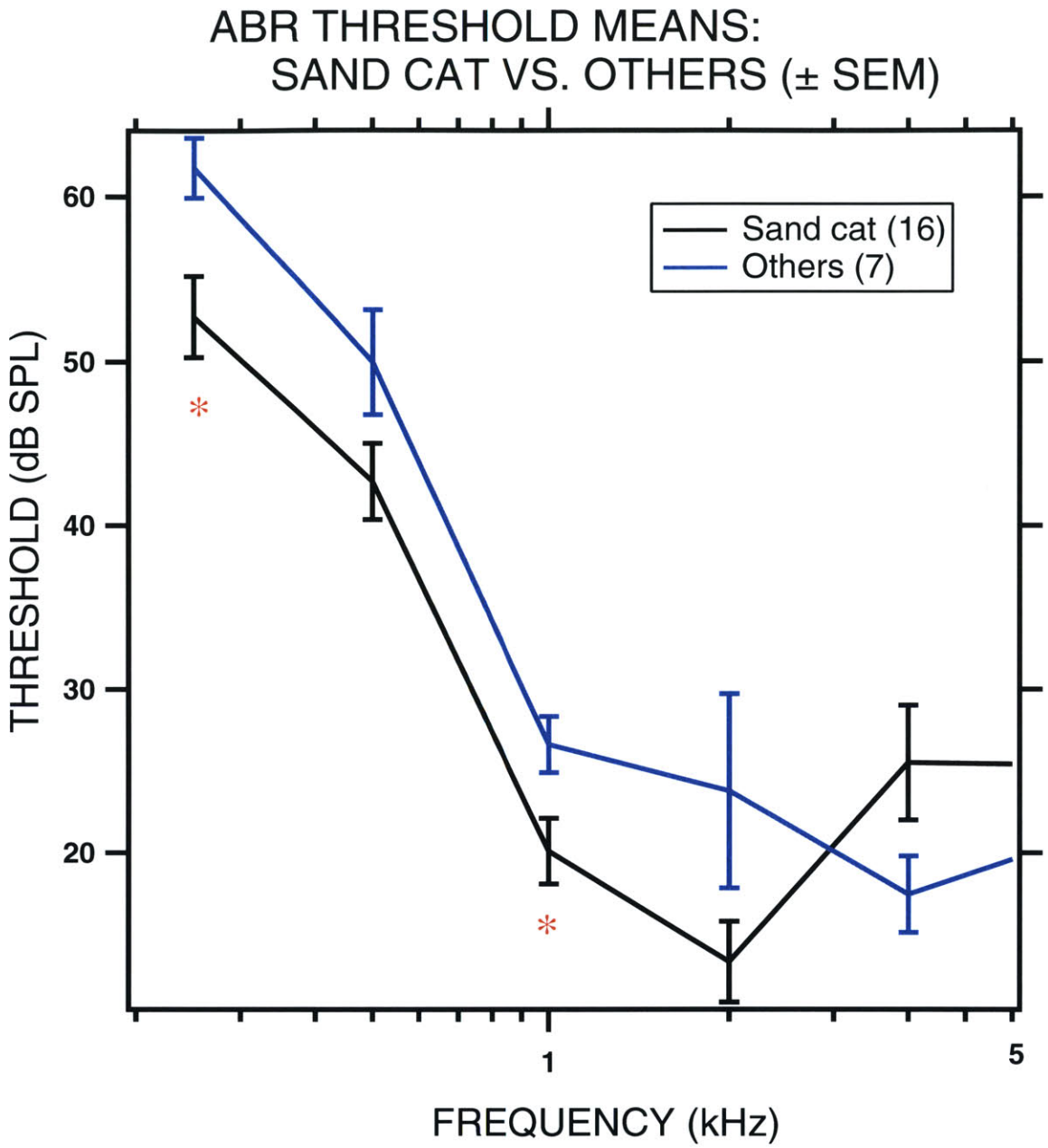

Figure 3.9: Threshold means determined from auditory brainstem responses for sand cats and non-sand cats groups. Threshold values for each specimen are determined at discrete frequencies an octave apart: 0.25, 0.5, 1, 2, and 4 kHz. The threshold values of sand cats are averaged at each frequency. The threshold values for the non-sand cat group are also averaged at each frequency. The vertical bars on the magnitude graph span mean ± SEM. An asterisk denotes a statistical difference with a 95% confidence level.

3.4 Correlation Between Acoustic Input Admittance and Threshold Values

Huang et al. (2002) assumed that if the efficiency of power transmission through the middle ear and the sensitivity of the inner ears and the central nervous system are equal across species, then higher acoustic power absorbed at the input of the middle ear would determine a lower hearing threshold. To test this hypothesis, we tried to test for correlation between the admittance data and the hearing threshold data. Overall, correlations are not significant between the input-acoustic admittance and threshold values across species at the frequency range of interest (<1 kHz, more specifically at 0.25, 0.5, 1 kHz). There is, however, a positive correlation of 1.6 with an $R^2 = 0.76$ between acoustic admittance magnitude and threshold value across four species at 4 kHz, which is in the opposite direction to the assumption.

4 Discussion

4.1 Overview

We attempt to answer two questions in this thesis: (1) Is sand cat hearing more sensitive than the hearing of other species? (2) Is interspecies sensitivity correlated to input admittances at the TM? To answer these questions, we used the same sound source in the ear canal to measure acoustic input admittance and to determine thresholds of auditory brainstem responses. Because the sample of non-sand cat species included 1 to 3 ears per species, we grouped the other species together. The resulting acoustic measurements are consistent with specialized acoustic characteristics (presumably as a result of specialized structure) within the sand cat. The results found in power absorption across the felid species are contrary to the idea that hearing sensitivity is dependent on the input to the tympanic membrane. Because of the arbitrary make-up of the non-sand cat group, we are not able to make quantitative assessment of interspecies differences.

4.2 Comparisons

4.2.1 Acoustic System

The acoustic system used in gathering acoustic data is a modification of that used in Huang et al. (2000). In Huang et al. (2000), the theoretical admittances were accurately measured up to around 8 kHz, where the limit for the current system is 5 kHz. The decreased accuracy at high frequency is most likely due to an increase in the crosstalk

artifact, within the ER10C. Although this restriction in frequency range removed frequencies of interest, we are still able to make interspecies comparisons in the low frequency range of special interest.

4.2.2 Comparisons of Acoustic Admittance of Sand cats (Table 4.1 and Figure 4.1)

Comparisons between our sand cat means and the Huang et al. (2002) show no statistical differences in magnitude. The angles show a statistical difference at 4 kHz. The Huang et al. data set, collected in 1999 also at The Living Desert, included 8 sand cat ears. It seems likely that their difference is a consequence of the general problem we have in making accurate measurements at high frequencies. Our data set contained 19 sand cat ears, with the right ear of Mukha common to both data sets.

Table 4.1: Statistical Difference for Sand cat Y_{TM}: Chan vs. Huang

	Magnitude			Angle		
Frequency (kHz)	Statistical Difference (95% confidence)	t Stat	P(T<=t) two tail	Statistical Difference (95% confidence)	t Stat	P(T<=t) two tail
0.125	N	0.460	0.6501	N	0.534	0.6077
0.25	N	-0.696	0.5000	N	-1.714	0.1095
0.5	N	-0.862	0.4071	N	-0.573	0.5784
1	N	-0.819	0.4364	N	-0.863	0.4066
2	N	-1.420	0.1749	N	1.471	0.1633
4	N	-0.510	0.6225	Y	-2.403	0.0351

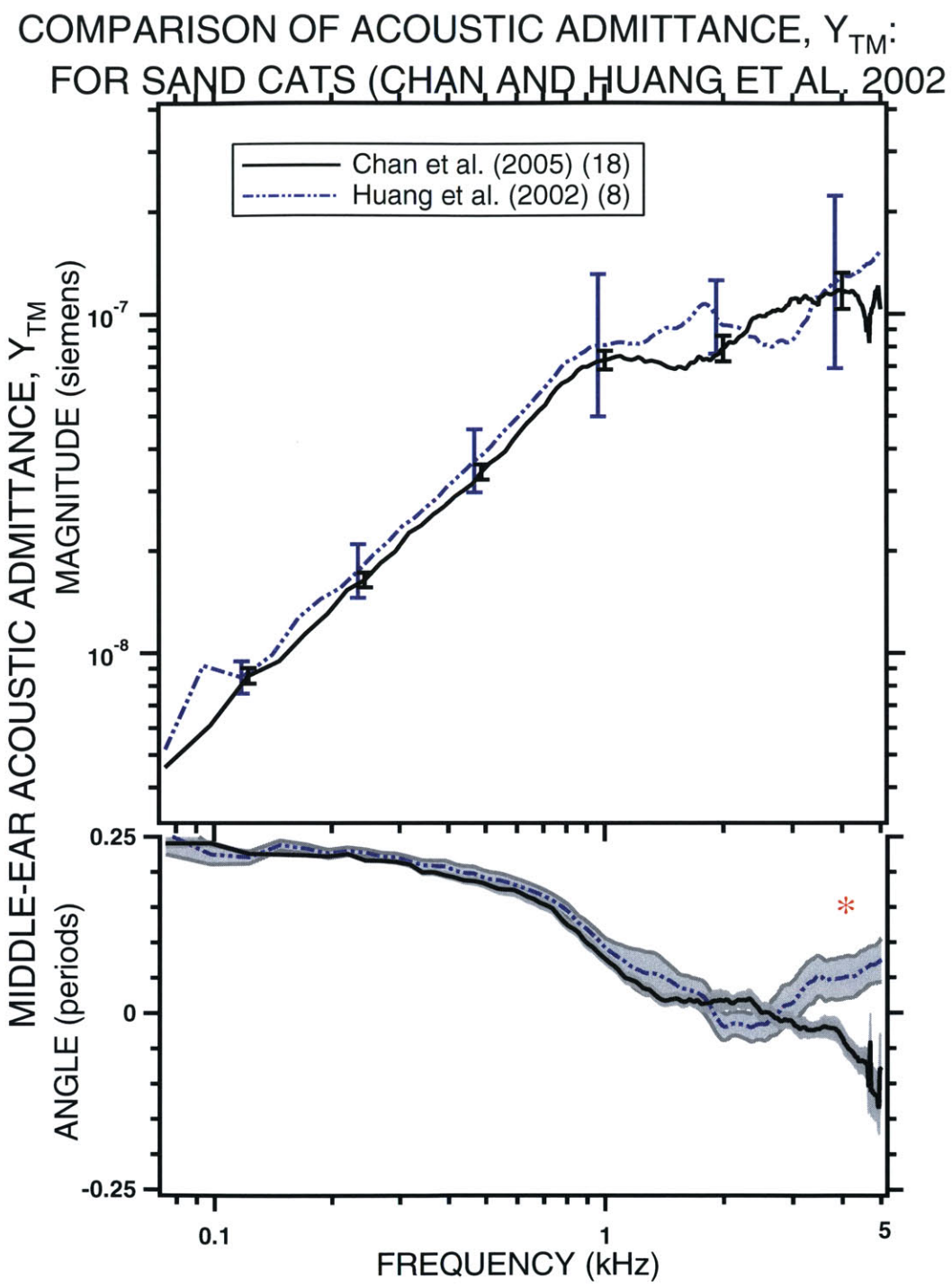

Figure 4.1: Comparison of Y_{TM}'s between 18 sand cat ears made in 2004 (Chan) and 8 sand cat ears made in 1999 (Huang et al.). The vertical bars on the magnitude graph span mean ± SEM at 0.125, 0.25, 0.5, 1, 2, and 4 kHz, which are the frequencies at which ABR threshold values were determined. On the angle plot, the one-standard-error range about the mean is shaded over the entire frequency range. The admittance magnitude curve for Huang data has been shifted by -50 Hz in order to distinguish ±SEM. The asterisk indicates that the mean angles at 4 kHz are significant at the 5% level.

4.2.3 $|Y_{TM}(f)|$ Notch

The notch frequency in felid ears is a frequency between 2 and 5 kHz (Huang et al. 2000) where acoustic admittance has a sharp drop in magnitude. This notch has been shown to be caused by a resonance in the cavities introduced by the septum that divides the air space and foramen that connects them (see Figure 1.4). Huang et al. (2000) demonstrates evidence for notches in all of the measured species except for one sand cat. Huang et al. (2002), with a larger sand cat sample, did not detect a notch in any sand cat ears. In this work, neither the sand cats nor the Arabian wildcats, both small species, show a clear notch. It is possible that the two felid species have notches at frequencies outside of our measured frequency range.

4.3 Trends

4.3.1 Body Size

With the exception of sand cats, the admittance magnitude of the felid species measured increase with body mass at frequencies less than 0.8 kHz. The mean body mass of measured species from smallest to largest are in the following order: sand cat, Arabian wildcat, bobcat, caracal, and serval. Below 0.5 kHz, the admittance magnitude of the individual species follows the body mass trend, except for the sand cat. The mean $|Y_{TM}|$ of the sand cats are about a factor of 1.5 higher than the mean of the servals, which is the largest felid measured with a mass 4 times that of the sand cat. The mean $|Y_{TM}|$ of the sand cat are a factor of 2.5 higher than that of the Arabian wildcat, which is the closest

felid in terms of body size with a mass 2 times that of the sand cat. These results are consistent with the data found in Huang et al. (2000).

4.3.2 Acoustic Power Absorption

The power absorbed at the tympanic membrane by an average sand cat ear is not significantly different from that absorbed by the average non-sand cat group. This result does not support the assumption that sand cats' specialized features, such as larger tympanic membrane and auditory bullae, make its ears absorb more acoustic power (for a given P_{TM}) than the average of other species in our sample. A contribution to the lack of difference is that sand cat's admittances angles are closer to 0.25 periods over the low frequency range (e.g. up 0.5 kHz). This compliant quality at the tympanic membrane can be characterized as elastic or spring-like, which means a large fraction of the energy delivered to the TM is returned to the system every cycle.

4.3.3 Hearing Thresholds

The ABR thresholds of sand cats are significantly lower than the non-sand cat group at 0.25 and 0.5 kHz. With the assumption that ABR thresholds are an indication of behavioral thresholds, the sand cat has higher hearing sensitivity than the average of the other felid species measured. Comparisons between hearing thresholds of individual species are difficult because of the limited number of species within our dataset. With the exception of the caracal, our data indicates that hearing threshold also increase with body size at low frequencies across measured species. The reason for this connection between ordering of hearing sensitivity and body size is unclear.

4.4 Connection Between Power Absorption and Hearing Sensitivity

The hypothesis of Huang et al. (2002) that motivated this thesis was that higher power absorption at the tympanic membrane implied a greater sensitivity to sound of the auditory system. Our data indicate that the average sand cat does not have greater power absorption at the tympanic membrane than the average of other measured species, but does have lower ABR thresholds and therefore are more sensitive to sound than the average of the non-sand cat group. This does not support the hypothesis that hearing sensitivity across species is correlated with acoustic power absorption.

The ear can be viewed as the external, middle, and inner ear as three cascading system. The vibrations of the tympanic membrane act as the input to the middle ear while the neuro-electrical impulses on 30,000 nerve fibers as the output of the inner ear. Input-admittance does not give us a transfer function of these systems, thus does not describe the input to the inner ear or the nervous system. Interspecies variations in other components could account for the sensitivity difference. Possible explanations could be:

Explanation 1a: Variations in middle ear mechanisms influence the sensitivity of the middle-ear system. Acoustic input admittance does not completely characterize signal transmission in the middle ear. Variations in mechanisms, like shape of the incus and stapes, influence the performance of the middle ear beyond the tympanic membrane. A change in structure could influence the tension in the ligaments and the muscles that suspend the ossicles chains, the lever and area ratios between the malleus and the stapes,

the motion of the round window and stiffness of the ossicular chain. Many of these factors have been shown to influence performance in the middle ear of human and could play a role in acoustic signal transmission from the tympanic membrane to the inner ear.

Explanation 1b: Variations in inner ear mechanisms influence the sensitivity of the inner-ear system. Acoustic admittances at the tympanic membrane capture little of inner ear function. Auditory brainstem response captures only the output of the inner ear. In kangaroo rats, it was shown that not only did the species have specialized middle structure but the species also had specialized cells in the cochlea (although no specialized function was discussed, Webster and Webster 1984). Variations in inner ear structures, like hair cell size, number of hair cells, the viscosity of inner ear fluid, could influence the signal transmission between the tympanic membrane to the brain. In this thesis, we focused on variations in the middle ear, which certain does not preclude any variation in the inner ear.

Explanation 2: Power absorbed at the tympanic membrane might not be the quantity that the rest of the auditory system is responsive to. The size of inner ear response is determined by the input magnitude of the stapes velocity to the round window. If a species gets bigger and $|Y_{\text{INNER EAR}}|$ increase, $|U_{\text{STAPES}}|$ will have to increase in order to keep the pressure of the inner constant. It could be the case that the middle-ear and inner-ear system itself are not varied (Explanation 1a and 1 b) but rather the input/output relationships between systems are responsible for hearing sensitivity (i.e. input admittance to the round window).

Bibliography

Beranek, L. (1996) Acoustics. Woodbury: American Institute of Physics, Inc.

Darwin, C. (1839) The Voyage of the Beagle. London: Penguin Books. (republished in 1989)

Dragesco-Joffé, A. (1993) La vie sauvage au Sahara. Lausanne: Delachaux et Niestlé S.A.

Herrington, S. J. (1985) Phylogenetic relationship of the wild cats of the world. PhD dissertation, University of Kansas, University Microfilms International, Ann Arbor, Michigan

Huang, G. T., Rosowski, J. J., and Peake, W. T. (2000a) Relating middle-ear acoustic performance to body size in the cat family: measurements and models. J Comp Physiol A 186:447-465

Huang, G. T., Rosowski, J. J., Puria, S., and Peake, W. T. (2000b) A noninvasive method for estimating acoustic admittance at the tympanic membrane. J Acoust Soc Am 108:1128-1146

Huang, G. T., Rosowski, J. J., Puria, S., and Peake, W. T. (2000c) Test of some common assumptions of ear-canal acoustics in cats. J Acoust Soc Am 108:1147-1161

Huang, G. T., Rosowski, J. J., Ravicz, M. E., and Peake, W. T. (2002) Mammalian ear specialization in arid habitats: structural and functional evidence from sand cat (*Felis margarita*). J Comp Physiol A 188:663-681

Kinsler, L. E., Frey, A. R., Coppens, A. B., and Sanders, J. V. (1982) Fundamentals of acoustics, 3rd edition. New York: Wiley

Rosowski, J. J. (2003) The Middle and External Ears of Terrestrial Vertebrates as Mechanical and Acoustic Transducers. Sensors and Sensing in Biology and Engineering: 59-69

Rosowski, J. J., Carney, L. H., and Peake, W. T. (1988) The radiation impedence of the external ear of cat: Measurements and applications. J Acoust Soc Am 84:1695-1708

Rosowski, J. J. and Graybeal, A. (1991) What did Morganucodon hear? Zoological Journal of the Linnean Society, 101:131-168

Schodde, Richard (1982) The Fairy-Wrens, A Monograph of the Maturidae. Melbourne: Lansdowne Editions:15-16

Seidensticker, J. and Lumpkin, S. (1991) Great cats: majestic creatures of the wild. Emmaus: Rodale Press

Silwa, A. (1999) Stalking the black-footed cat. Int Wildl May/June:38-43

Walsh, E. J., McGee, J., and Javel, E. (1986) Development of auditory-evoked potentials in the cat. I. Onset of response and development of sensitivity. J Acoust Soc Am 79:712-724

Webster, D. B. and Webster, M. (1972) Kangaroo rats auditory thresholds before and after middle-ear reduction. Brain Behav Evol 5:41-53

Webster, D. B. and Webster, M. (1984) The Specialized Auditory System of Kangaroo Rats. Contrib Sens Physiol 8:161-196

Wever, E. G. and Lawrence, M. (1954) Physiological Acoustics. Princeton: Princeton University Press: 2

Wonzencraft, W. C. (1993) Order Carnivora. In: Wilson DE, Redder geographic reference, 2nd edition. Washington DC: Smithsonian Institution Press, p279